Thesis for the Master's degree

Electrochemical advanced oxidation of toxic wastewaters using highly catalytic dimensionally stable anode and boron doped diamond electrodes

Advisor : Professor, Kyu-Jung Chae

Feb. 2019

Graduate School of Korea Maritime and Ocean University
Department of Civil & Environmental Engineering
Wan-Cheol Cho

Electrochemical advanced oxidation of toxic wastewaters using highly catalytic dimensionally stable anode and boron doped diamond electrodes

복합촉매 dimensionally stable anode 와 boron doped diamond 전극을 이용한 유해화학폐수의 전기화학적 고도산화 처리

Electrochemical advanced oxidation of toxic wastewaters using highly catalytic dimensionally stable anode and boron doped diamond electrodes

By
Wan-Cheol Cho

Department of Civil & Environmental Engineering
Graduate School of Korea Maritime and Ocean University

A thesis submitted to the faculty of the Korea Maritime and Ocean University in partial fulfillment of the requirements for the Master's degree in Department of Environmental Science and Engineering.

Busan, Republic of Korea
2018. 11. 27.
Approved by

Professor, Kyu-Jung Chae
Thesis Advisor

Accepted in partial fulfillment of the requirements for the Master's degree

Committee member : Prof. Young-Chae Song _____

Committee member : Prof. Jae-Soo Chang _____

Committee member : Prof. Kyu-Jung Chae _____

November. 27. 2018

Graduate School of Korea Maritime and Ocean University

Table of contents

List of Figures

List of Tables

Abbreviations

AOP, advanced oxidation process

BDD, boron-doped diamond

BET, Brunauer Emmett Teller

DSA, dimensionally stable anode

EAOP, electrochemical advanced oxidation process

EDX, energy dispersive X-ray spectroscopy

FE-SEM, field-emission scanning electron microscope

FID, flame ionization detector

GC, gas chromatography

HPLC, high performance liquid chromatography

PAH, polycyclic aromatic hydrocarbon

PGM, platinum group metal

SEM, scanning electron microscope

VOC, volatile organic compound

Electrochemical advanced oxidation of toxic wastewaters using highly catalytic dimensionally stable anode and boron doped diamond electrodes

Wan-Cheol Cho

Department of Civil & Environmental Engineering
Graduate School of Korea Maritime and Ocean University

Abstract

Electrochemical advanced oxidation processes (EAOPs) are a wastewater treatment process suitable for the treatment of degradable pollutants based on various oxidizers produced by direct and indirect oxidation. The material of anode is the most important in operating the EAOP. Three kinds of single catalyst DSAs (Ir/Ti, Pt/Ti and Ru/Ti) and four kinds of composite catalyst DSAs (Ir-Pt/Ti, Ir-Ru/Ti, Ir-Pd/Ti and Ir-Pt-Pd/Ti) and BDD anode were fabricated to evaluate oxidizer generation characteristics and pollutant removal characteristics based on each anode materials. The characteristics of the anodes were evaluated at the same current density of 25 mA/cm^2 at NaCl electrolyte. The oxidant generation characteristics were evaluated by comparing the amount of oxygen generated in the pollutant oxidation and the amount of generated · OH and ClO^- by the electrode reaction. The removal efficiencies for volatile organic

compounds (VOCs) wastewater and 1,4 dioxane were examined. In case of the BDD and Pt/Ti anodes, the ·OH generation reaction occurs more actively than the oxygen side reaction while ClO^- generation reaction occur slowly. For the DSAs without for Pt/Ti, the ·OH generation reaction occurred slowly, whereas the ClO^- generation reaction occurred rapidly. On the other hand, in the case of the composite catalyst DSA, the combination of Ir and Pd proved to be effective in improving the ·OH generation reaction. The removal efficiency of VOCs in Ir-Pd/Ti anode was the highest at over 80% and the rate of volatilization was less than 4.4%, which was the lowest among Ir-based composite catalyst DSAs. BDD and Pt/Ti anodes exhibited more than 90% of removal efficiency for 1,4-dioxaneas ·OH generation reaction occurs actively. This value is more than 60% higher than the other anodes, indicating that 1,4-dioxane is selectively removed through ·OH. This study implies that examination of oxidant generation of the electrode and development of the anode material based on the pollutant removal mechanisms will significantly improve treatment efficiency of EAOPs.

Key words: Electrochemical advanced oxidation; Dimensionally stable anodes; Platinium group metals; Boron-doped diamond electrode; Volatile organic compounds; 1,4-dioxane

복합촉매 dimensionally stable anode와 boron doped diamond 전극을 이용한 유해화학폐수의 전기화학적 고도산화 처리

조 완 철

한국해양대학교 대학원

토목환경공학과

초록

전기화학적 고도산화 공정은 직·간접산화에 의해 생성되는 다양한 산화제를 바탕으로 난분해성 오염물질 처리에 적합한 폐수처리공정이다. 산화전극의 소재는 전기화학적 고도산화 공정을 운영하는데 있어서 가장 중요 전극이다. 본 연구에서는 전극 소재에 따른 산화제 발생 특성과 오염물질 제거 특성을 평가하기 위해 세 종류의 단일 촉매 DSA(Ir/Ti, Pt/Ti, Ru/Ti)와 네 종류의 복합 촉매 DSA(Ir-Pt/Ti, Ir-Ru/Ti, Ir-Pd/Ti, Ir-Pt-Pd/Ti), BDD 전극을 제작하였다. 전극의 종류별 특성평가는 동일하게 NaCl 전해조건에서 25mA/cm^{2}의 전류밀도에서 수행되었다. 산화제 발생 특성평가는 오염물질 산화에 불필요한 산소 발생량과 전극 반응에 의해 생성되는 ·OH, ClO^-발생량을 비교하여 진행하였으며, 오염물질의 제거특성은 휘발성유기화합물 폐수와 1,4-다이옥산의 제거효율을 비교하여 평가하였다. BDD 전극과 Pt/Ti 전극은 산소 발생 부반응과 ClO^-의 발생반응이 느리게 일어나는 것에 비해 ·OH 발생반응은 활발하게 일어나는 것으로 나타났다. 또한, Pt/Ti를 제외한 DSA 전극은 ·OH 발생반응이 느리게 일어나는 반면에, ClO^- 발생반응은 빠르게 일어나는 것을 확인할 수 있었다. 한편, 복합촉매

DSA의 경우 Ir과 Pd를 조합하는 것이 ·OH 발생반응 향상에 효과가 있는 것으로 나타났다. 전극의 수명 측면에서 우수한 특성을 보이는 Ir을 기반으로 만든 복합촉매 DSA를 이용하여 휘발성유기화합물을 처리하였을 때, Ir-Pd/Ti 전극의 제거효율이 80% 이상으로 가장 높았을 뿐만 아니라 휘발되는 비율이 4.4% 미만으로 가장 낮은 것으로 나타났다. 한편, 1,4-다이옥산은 ·OH 발생반응이 활발하게 일어나는 BDD와 Pt/Ti 전극의 경우에만 90% 이상의 제거효율을 나타냈다. 이는 타 전극에 비해 60% 이상 뛰어난 것으로 1,4-다이옥산이 ·OH를 통해 선택적으로 제거되는 것으로 나타났다. 이와 같은 연구결과를 바탕으로, 전기화학적 고도산화 공정의 처리효율을 향상시키기 위해서는 전극 촉매 조합에 따른 산화제 발생 특성 연구와 오염물질의 제거기작에 기초한 전극 소재의 적용이 필요할 것으로 판단된다.

주제어: 전기화학적 고도산화, Dimensionally stable anodes (DSAs), 백금족 금속, Boron doped diamond electrode (BDD), 휘발성유기화합물, 1,4-다이옥산

Chapter 1. Introduction

The increase of toxic organic materials in water pollution is a worldwide concern due to the high resistance of these materials to traditional treatment methods, such as coagulation, biological oxidation, adsorption, ion exchange, and chemical oxidation (Zollinger, 2003;Sharma et al., 2007). These materials have been discharged in lakes, rivers, and oceans without an environmentally acceptable treatment option. This discharge causes serious environmental health problems in living organisms, including humans (Damalas and Eleftherohorinos, 2011).

Toxic wastewater contains various kinds of volatile organic compounds (VOCs), polycyclic aromatic hydrocarbons (PAHs) and heavy metals that are emitted from companies manufacturing petrochemical, food, medicine, wood and paper (Cheng et al., 2008; Jmaly et al., 2015; Kanakaraju et al., 2018). Such organic pollutants are difficult to remove because they are mixed in the wastewater with different decomposition mechanisms. Therefore, the toxic wastewater is treated by the advanced oxidation processes (AOPs) using ozone (O_3), hydrogen peroxide (H_2O_2), hydroxyl radical (· OH) and ultraviolet (UV) with strong oxidizing power. However, AOPs have a high power and maintenance cost, and lacks the ability to remove complex toxic chemicals. For this reason, toxic wastewater treatment requires an alternative, such as an electrochemical treatment, that is economical and can effectively treat volatile organic compounds (Lee et al., 2005).

There is great diversity within the electrochemical treatment approaches, such as electro-coagulation, electro-cementation, electro-floatation and electrochemical advanced oxidation (Curteanu et al., 2014;Palma-Goyes et al., 2015; Ahmadzadeh et al., 2017). The unique advantages of

electrochemical advanced oxidation processes (EAOPs), including simplicity, high efficiency, environmental friendliness, and cost-effectiveness, enable to be the most effective treatment techniques because coagulated or floated sludge are not generated from the process treatments are unnecessary.

Many forms of EAOPs have been investigated with various selectivity and reaction rates, that is accomplished as a result of direct and/or indirect oxidation on the electrode surface, such as electro-Fenton oxidation, photocatalytic oxidation, and electrochemical advanced oxidation (Moreira et al., 2017). Electro-Fenton oxidation, a well-known electrochemical process, but requires excessive Fe^{2+} concentration and produces a significant amount of chemical sludge during treatment (He and Zhou, 2017). Moreover, photocatalytic oxidation limits to a low organic pollutant degradation rate over a narrow photocatalytic region and a small fraction (<5%) of solar irradiation absorbance (Dong et al., 2015). However, electro-oxidation can degrades pollutants rapidly and non-selectively without producing sludge (da Silva et al., 2013; Särkkä et al., 2015; An et al., 2017).

Electro-oxidation reactions mainly depend on the electrochemical oxidizing agents, such as ·OH, H_2O_2, O_3, ClO^- ,and ClO_2^-, that have the ability to oxidize the organic compounds to the simplest structure such as CO_2 without secondary pollution (Rivera-Utrilla et al., 2013). The oxidation reaction mechanism can be classified as a direct or indirect mechanism. For direct mechanisms, the organic pollutants are selectively oxidized on the active oxidation sites of the metal, acting as an oxidizing agent with high oxidation potentials. In contrast, the indirect mechanisms occurs when the electrodes have no active oxidation sites, using other oxidized agents generated from the supporting electrolyte solution, such as hydroxyl radical groups or chlorine species (Basha et al., 2009;Curteanu et al., 2014; Rahmani et al., 2015; Murillo-Sierra et al., 2018).

There are many factors affecting the generation and concentration of the oxidants' agents, such as the electrode properties, pH, electrolyte type, electrolyte concentration, current density, and temperature (Moreira et al., 2017). Electrode materials are still the most important due to its direct connection between their active surface and the oxidant agent materials. As a result, most researchers seek to develop novel, effective, low-cost, and appropriate electrode materials to increase the efficiency in removing pollutants from wastewater solutions (López Peñalver et al., 2013; Rivera-Utrilla et al., 2013). PbO_2 and SnO_2 were investigated as an effective oxidizing-agent anodes with high oxidation potentials (oxygen evolution over potential 1.9 V); however, their low corrosion resistance, particularly with regard to chloride content, is a major drawback for these electrodes (Cossu et al., 1998; Anglada et al., 2009). When graphite was used as an anode, they exhibited low performance and poor ability during the electro-oxidation process due to their lower oxygen evolution potentials of 1.6 and 1.7 V, respectively (Pulgarin et al., 1994). Platinum group metal (PGM) electrodes have also been studied as high oxygen potential anode materials (2.7 V), and the obtained results confirmed they were dimensionally stable with excellent performance; however, their high cost and short lifespans restrict their application (Britto-Costa and Ruotolo, 2012; Martins et al., 2012). PGMs that can be used as an oxidation catalyst are platinum (Pt), ruthenium (Ru), iridium (Ir), and palladium (Pd), that are known to have different electrochemical characteristics and lifetimes for each material (Park et al. 2016). Although electrode materials are reported to have different electrochemical properties depending on the contaminants to be treated, Ir is known to be superior for electrode lifetime (Yi et al., 2007). For this reason, Ir is commonly used in EAOPs, but they suffer from poor electrochemical characteristics due to low oxygen overvoltage (Pulgarin et

al., 1994). Modified titanium electrodes with a thin layer of ruthenium dioxide (RuO_2/Ti) have been presented as promising electrode materials for organic pollutant degradation of wastewater effluents (Chae et al., 2004; Yavuz and Koparal, 2006; Hamida et al., 2017). The cost-effective RuO_2/Ti electrode possesses good stability, a high oxygen evolution potential of 2.0 V (Anglada et al., 2009), chemical resistance, and high electrocatalytic activity for chlorine evolution and other strong oxidants (•OH, H_2O_2, and O_3) (Panizza and Cerisola, 2009). Pd is well known for its high electrochemical activity and thermal stability. Moreover, its high anode anti-poisoning effect improves catalytic anodic oxidation, while minimizing adverse electrode oxidation by oxygen molecules, as compared with other platinum group metals (Feng et al., 2016; Mahajan et al., 2017). In addition, studies have been conducted on composite catalytic metal electrodes using various platinum group metals for improved performance, and iridium is used as a base material to make up for the electrode lifetime advantages (Park et al., 2016). Recently, BDD (Boron-doped diamond) electrode, that has an excellent electrochemical reactivity based on high oxygen overvoltage, has been used in research for decomposing pollutants (Liu et al., 2018).

To examine the electrochemical high-level oxidation performance according to the electrode material, single-catalyzed DSAs (Ir/Ti, Pt/Ti, and Ru/Ti), Ir-base composite catalyst DSAs (Ir-Pt/Ti, Ir-Ru/Ti, Ir-Pd/Ti and Ir-Pt-Pd/Ti) and BDD/Ta electrode were fabricated. The prepared electrodes were evaluated for their electrochemical oxidation ability by comparing the amounts of oxidant generated and applying to VOCs and 1,4-dioxane wastewater treatment.

Chapter 2. Literature review

2.1 Electrochemical advanced oxidation

The electrochemical advanced oxidation is a technique to treat wastewater by using an oxidation reaction that occurs when an anode and a cathode are installed in a conductive liquid and a current is flowed. Electrochemical treatment of wastewater causes electron transfer reaction through the electrode as an intermediary. It is generally classified into direct reaction and indirect reaction.

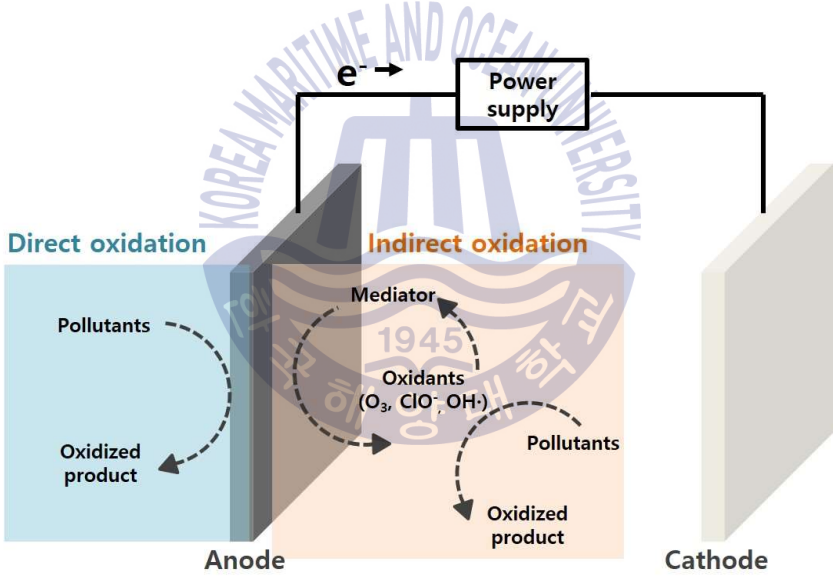

Fig. 2.1. A schematic showing direct and indirect electrochemical oxidation of pollutants.

As shown in Fig. 2.1, the direct reaction is adsorbed on the surface of the electrode to cause the electron transfer reaction, and the product is separated from the electrode. Indirect reactions are reactions using intermediates such as highly reactive compounds that

can facilitate electron transfer reactions. The intermediates may be regenerated by a reversible reaction and may cause an irreversible reaction (Lee et al., 2011).

2.1.1. Direct oxidation

In the EAOPs, ·OH is adsorbed on the surface of the anode (M) by strong physical adsorption as shown in Equation (1) (Moreira et al., 2017).

$$M + H_2O \rightarrow M(\cdot OH) + H^+ + e^- \quad (1)$$

However, when an electrode with low oxygen overvoltage is used, M(· OH) changes easily in the form of MO as shown in equation (2) (Moreira et al., 2017).

$$M(\cdot OH) \rightarrow MO + H^+ + e^- \quad (2)$$

M(· OH), as shown in Equation (3), causes the hydroxyl radical adsorbed on the surface of the oxidized electrode to convert organic pollutant (R) into carbon dioxide during the electrolysis process. MO oxidizes organic pollutants as shown in equation (4) (Park et al., 2016).

$$R + M(\cdot OH)_n \rightarrow CO_2 + nH^+ + ne^- + M \quad (3)$$

$$R + MO \rightarrow RO + M \quad (4)$$

On the other hand, hydrogen peroxide is generated by the reduction reaction of oxygen at the cathode as shown in equation (5) (Moreira et al., 2017; Franz et al., 2002).

$$O_2 + 2H^+ + 2e^- \rightarrow H_2O_2 \quad (5)$$

2.1.2. Indirect oxidation

M(·OH) can generate hydrogen peroxide (H_2O_2) as shown in equation (6), and ozone can be generated on the electrode surface as shown in equation (7) (Moreira et al., 2017).

$$2M(\cdot OH) \rightarrow 2MO + H_2O_2 \quad (6)$$

$$3H_2O \rightarrow O_3 + 6H^+ + 6e^- \quad (7)$$

In addition, various ROS (reactive oxygen species) having oxidizing power can be generated according to the combination of the electrolyte and the oxidizing electrode, which serve as a mediator through the EAOPs. DSAs made of PGMs are used to oxidize chlorine ion (Cl-) to chlorine (Cl2) as shown in Equatioin (8). The active chlorine in water is present as Cl2 under pH 3, HClO at pH 3-8, hypochlorite (ClO^-) above pH 8, as shown in equations (9) and (10) (Panizza and Cerisola, 2009)

$$2Cl^- \rightarrow Cl_2 + 2e^- \quad (8)$$

$$Cl_2 + H_2O \leftrightarrow HClO + Cl^- + H^+ \quad (9)$$

$$HClO \leftrightarrow ClO^- + H^+ \quad (10)$$

Also, ClO^- can be generated by the reaction of BDD electrode and chlorine ion as shown in equation (11) (Sánchez-Carretero et al., 2011).

$$Cl^- + \cdot OH \rightarrow ClO^- + H^+ + e^- \quad (11)$$

BDD electrode can be combined with electrolytes such as sulfate ion, phosphate ion and carbonate ion, so that strong oxidizing agents are generated as shown in equations (12), (13) and (14) (Cañizares et al., 2006).

$$2SO_4^{2-} \rightarrow S_2O_8^{2-} + 2e^- \quad (12)$$

$$2PO_4^{3-} \rightarrow P_2O_8^{4-} + 2e^- \quad (13)$$

$$2CO_3^{2-} \rightarrow C_2O_6^{2-} + 2e^- \quad (14)$$

2.2 Case study of wastewater treatment using EAOPs

Examples of wastewater treatment using EAOPs are summarized in Table 2.1.

Table 2.1. Examples on the treatment of wastewater using EAOPs.

Anode/ cathode	wastewater characteristics	Electrolyte conc.	Current density	Removal efficiency	Ref.
DSA (RuO_2/Ti) / stainless steel	phenolic wastewater (100 mg/L of 3,4,5-trimethoxybenzoic ,4-hydroxybenzoic, gallic, protocatechuic, trans-cinnamic and veratric)	NaCl (0.25 M) or Na_2SO_4 (0.07 M)	57 mA/cm^2	100% (180 min)	(Fajardo et al., 2017)
DSA (IrO_2-RuO_2/Ti) and SnO_2/ Pt	Dyeing wastewater (50 mg/L of Rhodamine B dye)	NaCl (0.05 M) and Na_2SO_4 (0.1 M)	20-40 mA/cm^2	86-96% (90 min)	(Baddouh et al., 2018)
DSA (Pt-Ru-Ir-Ti)/ stainless steel	Pharmaceutical wastewater (50 mg/L of creatinine)	NaCl (0.02 M)	10.29 mA/cm^2	81.25% (85 min)	(Singla et al., 2018)
PbO_2 and SnO_2-PdO_2-RuO_2/Ti /Stainless steel	Municipal sanitary landfill leachate (COD : 4100−5000 mg/L and BOD <1000 mg/L)	NaCl (0.3 M) and Na_2SO_4 (0.037M)	25-100 mA/cm^2	n.a.	(Chiang et al., 1995)
BDD/ stainless steel	Pharmaceutical wastewater (100 mg/L of Enrofloxacin)	Na_2SO_4, NaCl, Na_2CO_3, $NaNO_3$ or Na_3PO_4 (0.1 M)	10 mA/cm^2	30-88% (9 h)	(Carneiro et al., 2018)
BDD/ Ti	Mixture of secondary Municipal Wastewater Treatment plant and textile wastewaters after RO	Cl^- (16.7 M)	17 mA/cm^2	n.a.	(Van et al., 2002)

Anode/ cathode	wastewater characteristics	Electrolyte conc.	Current density	Removal efficiency	Ref.
DSA (Pt) or BDD/ stainless steel	Pharmaceutical wastewater (175 mg/L of diclofenac)	Na_2SO_4 (0.05 M)	17-150 mA/cm^2	100% (360 min)	(Brillas et al., 2010)
BDD/ Pt	Dyeing wastewater (315 mg/L of Indigo dye)	NaCl (0.07 M)	33-150 mA/cm^2	n.a.	(Nava et al.,2014)
BDD or Pt/ stainless steel	Dyeing wastewater (69-548 mg/L of Methyl Violet 2B dye)	Na_2SO_4 (0.05 M)	33-150 mA/cm^2	74% (60-600 min)	(Hamza et al., 2009)
DSA/ stainless steel	Real textile wastewater (COD : 5957 mg/L)	n.a,	10-100 mA/cm^2	n.a.	(Vaghela et al., 2005)
BDD/ stainless steel	Real pharmaceutical wastewater (COD : 12000)	n.a.	26-179 mA/cm^2	100	(Domínguez et al., 2012)

2.2.1 Electrode

The materials used for the anode are PbO_2, SnO_2, DSA and BDD, among which DSA and BDD electrodes are the most used. Ir, Ru, Pt, and Pd are materials that can be used as DSA, and Ir and Ru are most actively used for water treatment purposes. Cathode is used in various ways such as stainless steel, titanium, platinum. It is considered that it is difficult to compare the performance of all kinds

of electrodes because the properties and electrolysis conditions of the wastewater treated by each electrode are different.

2.2.2 Wastewater

Dyeing wastewater and pharmaceutical wastewater are the most frequently treated wastewater for EAOPs. The target wastewater is synthetic wastewater that is artificially injected with pollutants, and the concentration of pollutants is 5 to 500 mg/L. In addition, the actual wastewater used in EAOPs was found to contain textile wastewater, pharmaceutical wastewater, and landfill leachate. They were not only degradable but also had a high COD concentration of over 5000 mg/L. Also, the actual wastewater was suitable for operating the EAOPs, so that the electrolyte was not added.

2.2.3 Electrolytic conditions

As the electrolyte used in EAOPs, NaCl and Na_2SO_4 were most widely used, and Na_2CO_3, $NaNO_3$ and Na_3PO_4 were used for comparison between electrolytes. BDD electrodes had no electrolyte limitations, but the electrolyte was limited to chlorine ion (Cl^-) depending on the constituent materials of the DSA (Moreira et al., 2017). Electrolyte concentration was lower than 1 M in most cases. The current density was operated in the range of 10-180 mA/cm^2, and the operating time was set to be variable according to the decomposition of the pollutants.

Chapter 3. Assessment of oxidant generation

3.1 Introduction

Since the electrochemical characteristics depend on the electrode materials, the performance of EAOP and oxidant generation amount should be comparable to the electrode type. Although a wide variety of electrodes have been used to treat wastewater, most of the EAOPs research cases compare the wastewater treatment performance for 1-3 types of electrodes. Therefore, it is difficult to directly compare EAOPs performance and oxidant generation amount according to the electrode type.

As shown in equation (1), ·OH attached to the electrode surface in EAOPs not only decompose contaminants but also produce various ROS. On the other hand, Oxygen may be generated by the decomposition of water due to the electrode reaction as shown in equation (15). However, it does not contribute to the oxidation of pollutants, which hinders the operation of EAOPs (Lee et al., 2011; Franz et al., 2002)

$$2H_2O \rightarrow O_2 + 4H^+ + 4e^- \quad (15)$$

As mentioned in Chapter 2, BDD electrodes have no electrolyte limitations, but the electrolyte was limited to Cl^- depending on the constituent materials of the DSA. For direct comparison of the performance of DSAs and BDD, it is desirable to use an electrolyte containing Cl^- for the same electrolysis conditions. When Cl^- electrolytes are used for EAOPs, CLO^- is produced by equations (8-10) and (11).

In order to measure the amount of oxidant generated in EAOPs, it is necessary to measure the concentration of ROS. However, it is common for ROS to compare trends with probe materials that are selectively removed or bound to a specific ROS due to the absence of standardized concentration calibration methods (Gomes et al., 2005). As oxygen probe materials, substances such as furfuryl alcohol, 9,10-Dimethylanthracene and 9-[2-(3-Carboxy-9,10-diphenyl)anthryl]-6-hydroxy-3H-xanthen-3-ones are used (Gomes et al., 2005; Ray and Tarr, 2014). ·OH probes include sodium terephthalate, p-chlorobenzoic acid, Fluorescein and Coumarin (Gomes et al.; Khuntia et al., 2015). ClO^- is standardized as measured by N,N-Diethyl-phenylenediamine but it is not suitable at high concentrations and may be indirectly compared using absorbance at 200-350 nm using UV-visible spectroscopy.

This chapter describes the evaluation of the amount of oxidant generated in various types of DSA and BDD electrode. In order to evaluate the amount of oxidant generated, single catalytic DSA electrodes of Ir/Ti, Pt/Ti, Ru/Ti and composite catalytic DSA Ir-Pt/Ti, Ir-Ru/Ti, Ir-Pd/Ti and BDD electrode Respectively. The tendency of oxygen generation by side reaction was measured for each anode using furfuryl alcohol as a probe material. In order to examine the degree of direct oxidation and the tendency of ROS for each anode, indirect measurement was performed using pCBA as a probe material. In addition, ClO^- produced by the oxidation reaction of the electrolyte for each anode was indirectly compared using the absorbance in UV-visible spectroscopy.

3.2 Materials and methods

3.2.1 Electrode materials

The anode and cathodes were designed to have surface areas of 50 cm^2 (7.1 cm in length, 7.1 cm in width, and 0.1 cm in thickness) with fifteen holes (⌀ = 6 mm). The fabricated anode consists of three single catalytic DSAs, four composite catalytic DSA and BDD electrodes. The anode was made of a punctured Ti plate coated with a 3.0 μm-thin layer of different single catalytic PGMs (Ir, Pt and Ru) and composite catalytic PGMs (Ir-Pt, Ir-Ru, Ir-Pd and Ir-Pt-Pd). Each catalyst was used in an amount of 50 mg. As the base model of composite catalyst, Ir was used for its high chemical stability, with a weight of 90% of the total catalytic composites (45 mg of Ir and 5 mg of Pt, Pd, Ru or 2.5 mg of Pt and 2.5 mg of Pd respectively). Cathode was made of Pristine Ti. All the investigated electrodes were manufactured with the assistance of WESCO Electrodes Co. Ltd. (Republic of Korea).

3.2.2 Electrochemical reactor setup and its operation

All the experiments were conducted in a rectangular reactor made of an acrylic sheet (74 × 46 × 110 mm). The distance between the anode and cathode materials was maintained at 2 mm. A simplified diagram of the experimental setup is shown in Fig. 3.1. First, 300 mL of the 20 mM furfuryl alcoho as oxygen probe or 300 μM p-chlorobenzoic acid as ·OH probe with 0.05 M NaCl Solution was inserted into the electrolysis cell and mixed using a magnetic stirrer. The two electrodes were connected to a DC power supply, OPM-303D from ODA Co. (Republic of Korea), that was used for maintaining the current density at 25 mA/cm^2 during the electrochemical

advanced oxidation. The liquid samples were collected at 0, 5, 10, 15, 20, 25, and 30 min during the experiment.

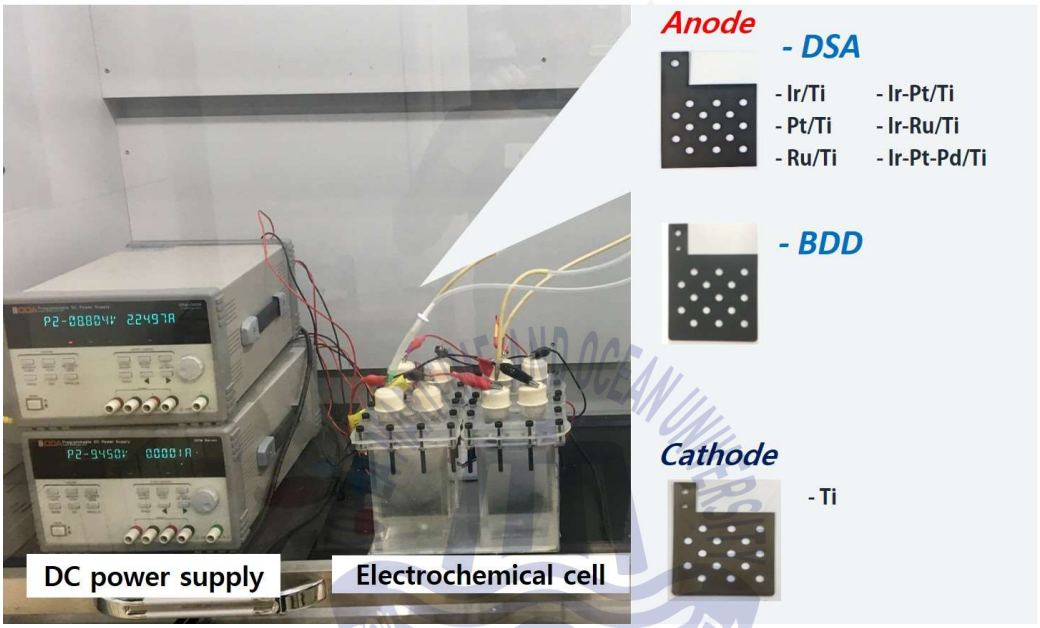

Fig. 3.1. The electrochemical advanced oxidation system (Batch type, 300mL of working volume).

3.2.3 Measurements

The concentration of furfuryl alcohol was analyzed using gas chromatography (GC) (Claus 580, PerkinElmer) with a flame ionization detector (FID, PerkinElmer) and a non-polar capillary GC column (Ultra-2, 25 m, 0.20 mm, Agilent). The analysis condition of the GC is shown in Table 3.1. A headspace sampler (Turbo matrix 40, Perkin Elmer) was used to pretreat the furfuryl alcohol solution before injection into the GC

analyzer.

Table 3.1. Organic matter analysis conditions for gas chromatography.

Parameter	value
Column flow	1.0 mL/min
Injection port temperature	200 ℃
Oven temperature	40 – 100 ℃ (15 ℃/min, 4 min)
Detector temperature	250 ℃
Carrier gas flow	2.0 mL/min (Nitrogen)
Detector gas flow	45 mL/min (Hydrogen) / 450 mL/min (air)

The concentration of p-chlorobenzoic acid concentration was analyzed using high performance liquid chromatography (HPLC) with a variable wavelength detector (G1314A, Agilent) and ZORBAX Eclipse Plus C18 (3.5 μm, 4.6 × 100 mm, Agilent) The condition of the HPLC charaterization is shown in Table 3.2.

Table 3.2. p-chlorobenzoic acid analysis conditions for high performance liquid chromatography.

Parameter	value
Injection volume	50.0 μL
Flow rate	1.5 mL/min
Mobile phase	45/55 (v/v) 10 mM phosphoric acid/methanol
Column temperature	30 ℃
Wavelength	234 nm

The degree of ClO^- generation was measured at intervals of 5 nm from 200 to 400 nm with UV-visible spectrometer (Optizen pop, Mecasys).

3.3 Results and discussion

3.3.1 Oxygen generation

During the operation of EAOPs, oxygen from the side reaction called water decomposition reaction gives negative effect on oxidizing ability (Lee et al., 2011; Franz et al., 2002). Oxygen generated during the operation of EAOPs for each anode was measured using a probe material, furfuryl alcohol. As shown in Fig. 3.2, as the consumption of furfuryl alcohol increased, the more oxygen was generated by the side reaction. Based on the removal tendency of the furfuryl alcohol (oxygen generation rate), the electrodes were divided into two groups: I) the faster removal rate of furfuryl alcohol: Ir/Ti, Ir-Pt/Ti, Ir-Ru/Ti, and Ir-Pd/Ti anodes belonged to the group, II) relatively slow removal rate: the Pt/Ti, Ru/Ti, Ir-Pt-Pd/Ti, and BDD anodes. The side reaction of Pt/Ti was the lowest and the BDD electrode, that was known to have excellent oxidizing power, and had a low degree of side reaction. As a result, it is considered that Ir catalyst is more specific to the oxygen evolution reaction than the other catalysts. However, Ir-Pt-Pd has different oxygen generation tendencies from other Ir catalyst containing DSAs. Ir-Pt-Pd/Ti had the same Ir catalyst ratio as other composite catalysts, but the rate of oxygen generation was twice as low. Therefore, it is possible to inhibit the side reaction through the combination of catalysts. On the other hand, when the purpose of the cathodic reduction reaction is to generate hydrogen peroxide using oxygen generated from the anode, the oxygen evolution reaction acts as a forward reaction (Ma et al., 2019). Therefore, it is necessary to study Ir catalyst in terms of cathodic reduction.

In order to compare the tendency of oxygen generation more intuitively, the results of comparing the amounts of furfuryl alcohol removed for 30

min are shown in Fig. 3.3.

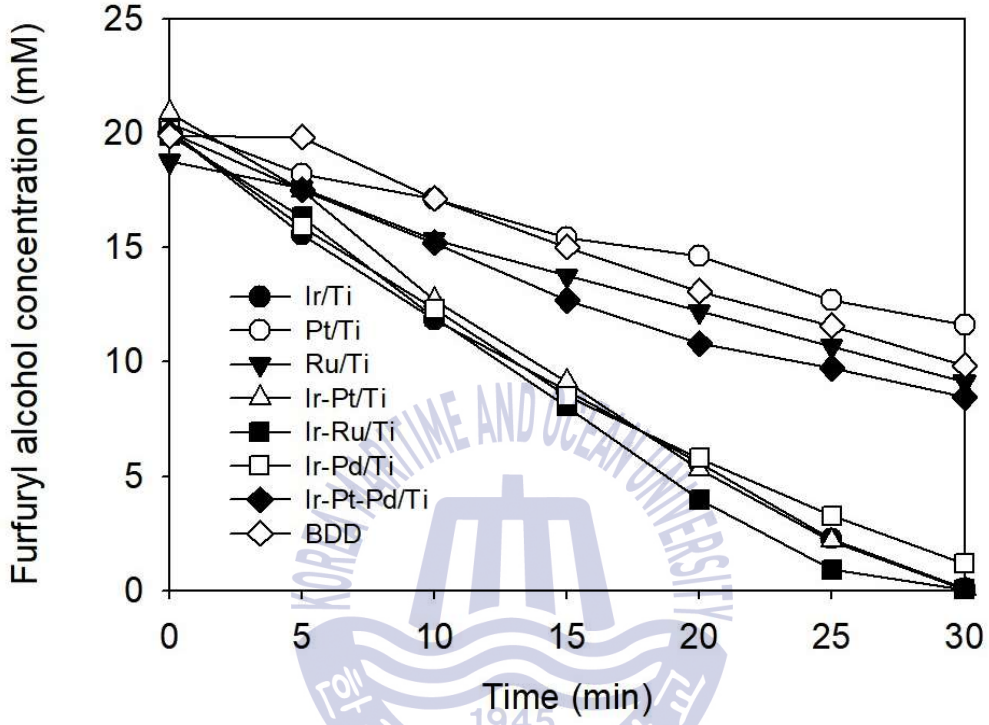

Fig. 3.2. Removal of furfuryl alcohol (oxygen probe) versus time on different anodes (25 mA/cm^2 and 0.05 M NaCl).

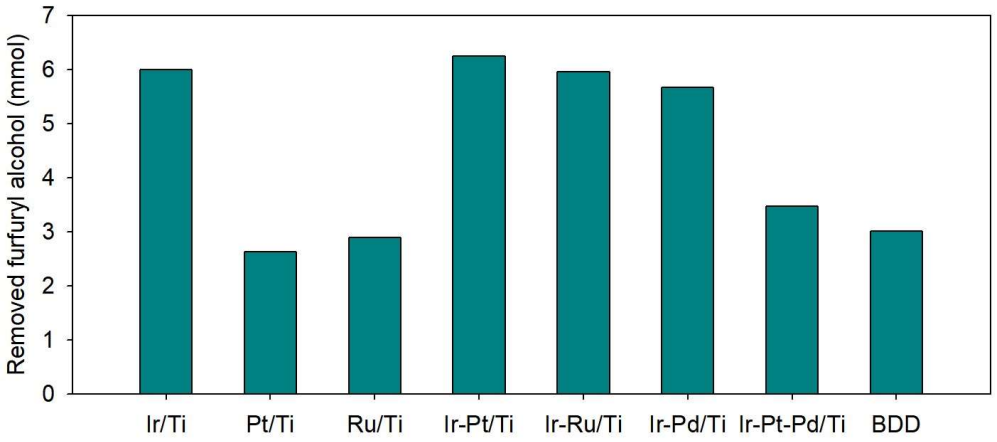

Fig. 3.3. Removed amount of furfuryl alcohol (oxygen probe) for 30 min (25 mA/cm^2 and 0.05 M NaCl).

3.3.2 ·OH genereation

·OH in EAOPs is a key material for performance evaluation of electrodes because it affects the direct degradation of contaminants and the production of various ROS. ·OH generated during the operation of EAOPs for each anode was measured using a probe material, p-chlorobenzoic acid. The results are shown in Fig. 3.4, as more p-chlorobenzoic acid was consumed the more ·OH was generated. The rate of ·OH formation of the BDD electrode was much faster than that of the DSA electrode. Pt/Ti produced ·OH at a rate two times slower than the BDD anode, while other DSAs generated at a much slower rate. In order to compare the tendency of ·OH more intuitively, the amounts of p-chlorobenzoic acid that was removed for 30 min are shown in Fig. 3.5. Ir/Ti produced the least amount of ·OH, while ·OH production slightly increased when the other metal and composite catalytic electrode were made. The Pt catalyst generated the highest amount of ·OH among the PGM catalysts

(individually), while the combination with Ir catalyst decreased ·OH generation was minimized. However, considering the amount of ·OH from Ir-Pd/Ti and Ir-Pt-Pd/Ti combination catalysts, Ir catalyst generated increased amount of ·OH when it was used in combination with the Pd catalyst. Therefore, the structural stability of Ir catalyst and the high ·OH generation amount can be expressed by controlling the composition of Ir and Pd catalysts.

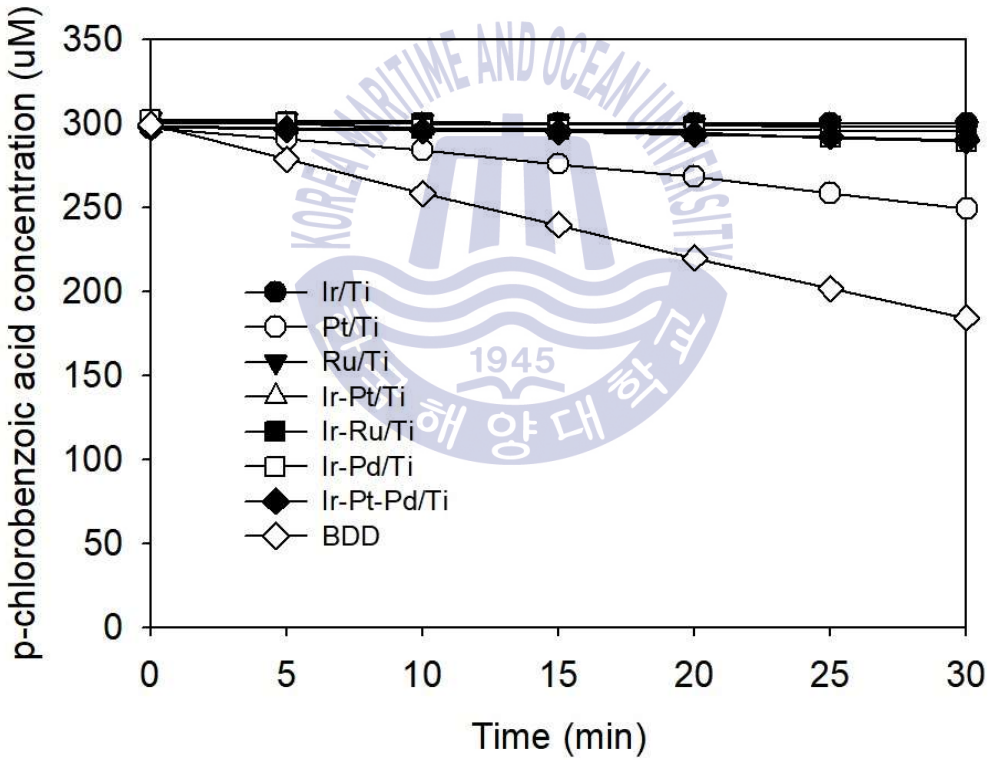

Fig. 3.4. Removal of p-chlorobenzoic acid (·OH probe) versus time on different anodes (25 mA/cm^2 and 0.05 M NaCl).

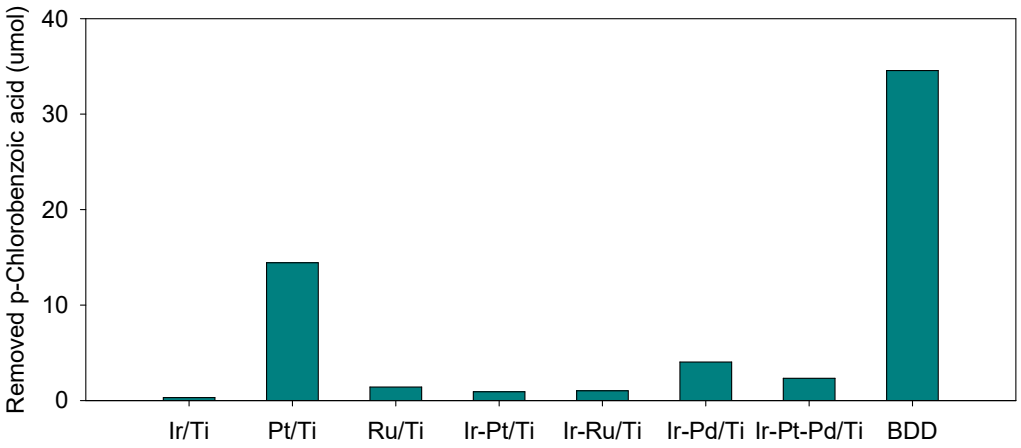

Fig. 3.5. Removed amount of p-chlorobenzoic acid (· OH probe) for 30 min on different anodes (25 mA/cm^2 and 0.05 M NaCl).

3.3.3 OCl^- genereation

NaCl as an electrolyte in EAOPs, produced ClO^- due to the electrode reaction (Moreira et al., 2017). ClO^- generated by each anode was measured by UV-visible spectroscopy 200-350 nm wavelength. The results in Fig. 3.6, higher absorbance at 250-350nm means the more ClO^- generation. Due to the exceeding value of some electrode for 20 min operation, the comparison of the degree of ClO^- generation by anodes for 20 min was determined to be impossible. In 15 min, Pt/Ti and BDD anodes generated ClO^- more than twice as much as the other anodes. In addition, the degree of ClO^- generation in the single catalytic DSAs was in the order of Ir/Ti > Ru/Ti > Pt/Ti. Composite catalytic DSAs exhibited a higher degree of ClO^- generation than single catalytic DSAs. Therefore, it is necessary to study chlorine generation from Ir based composite catalyst electrode such as ship ballast water treatment system (Särkkä et al., 2015). Among the composite

catalytic DSAs, Ir-Pd showed a higher degree of ·OH generation as well as ClO^- generation due to the relatively low side reaction activity.

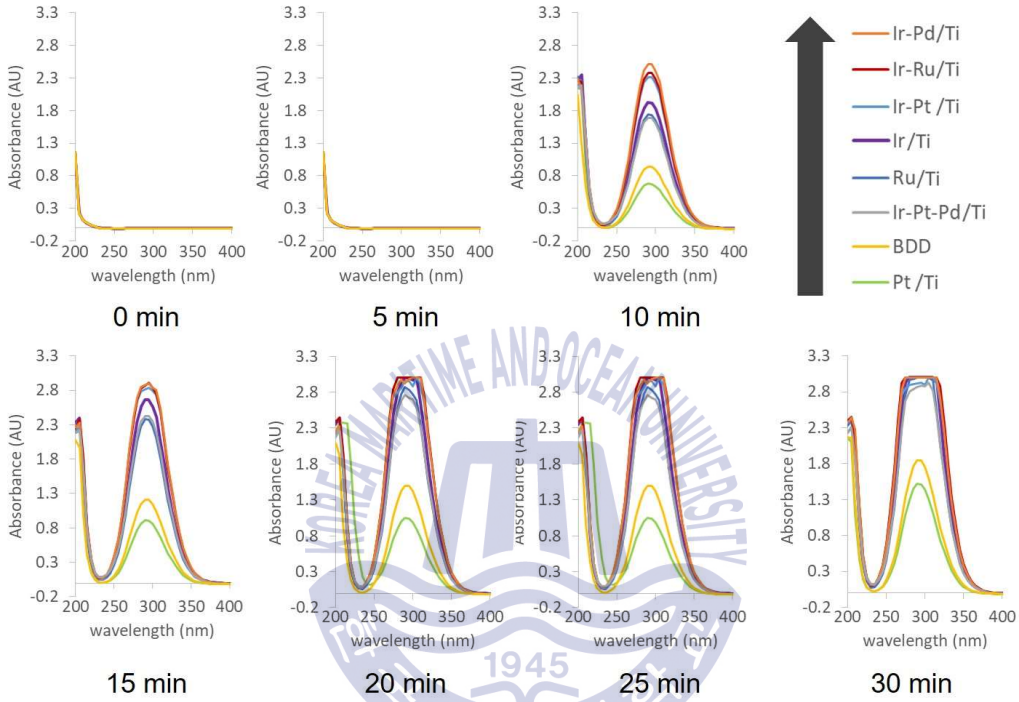

Fig 3.6. UV-visible absorbance at 200-400 nm with time-series electrodes on different anodes (25 mA/cm^2 and 0.05 M NaCl).

3.4 Conclusion

The electrochemical characteristics such as side reaction activity and oxidant generation were different depending on the type of the electrode under the same electrolysis conditions. In the NaCl electrolysis condition, the BDD anode had low side reaction activity and ClO^- generation was lower than DSA. However, it is considered that the BDD electrode has a high oxidizing power based on the excellent ·OH generation amount. Ir/Ti DSA exhibited high side reaction activity and excellent ClO^- generation, but showed very low ·OH generation ability. Ru/Ti DSA had similar activity to the Ir/Ti oxidant, while having less side reaction activity. Pt/Ti electrode had similar properties to the BDD anode, although the ·OH generating capacity did not reach the BDD electrode. Composite catalytic DSAs made of Ir base had properties similar to those of Ir, but the degree of ClO^- and ·OH formation increased. In particular, combination of Ir and Pd catalysts was found to be effective in accelerating ·OH generation. Therefore, it is expected that the performance of DSA electrode can be improved while maintaining the advantages of existing catalyst by various catalyst combination. In addition, Evaluation of the oxidant generation will enable to apply the suitable (appropriate) anode for the wastewater characteristics.

Chapter 4. VOCs wastewater treatment

4.1 Introduction

Volatile organic compounds (VOCs) are dangerous due to their toxicity, potential hazardous effects, and rapid evaporation to the atmosphere, which can create secondary air pollution (Mudliar et al., 2010; Pollack et al., 2013). Benzene, chloroform, trichloroethylene, and toluene are the most common VOC pollutants emitted by the different chemical and petrochemical industries, including petroleum refining, paint manufacturing, large steel-structure manufacturing, and automobile manufacturing (Cheng et al., 2008).

From an environmental point of view, it is important to remove VOCs and limit and control their vapor emissions to avoid their negative effects on climate change, plant growth, and human health. Over the past three decades, significant efforts have been exerted to develop more effective techniques for removing VOCs from wastewater. These techniques are basically classified into three different groups: physical treatment, such as air stripping, various membrane filtrations, and the adsorption process (Shah, 2004; Wu et al., 2004; Celebioglu et al., 2016) biological treatment, such as the aerobic/anaerobic treatment process (Easter et al., 2005; Mudliar et al., 2010) and electrochemical treatment (Moreira et al., 2017). In the electrochemical treatment process, electrical activity and chemical activity are integrated to achieve the highest removal percentage of undesirable organic pollutants.

In spite of the previously mentioned studies, none of them, to date, has addressed the optimum conditions for controlling the vapor emissions of

VOC pollutants in wastewater. This study introduces material groups with high dimensional stability as novel, effective oxidizing-surface sites; they are cost-effective, have anodes with long lifetimes, and are suitable for the degradation of VOCs from synthetic wastewater via the electrochemical advanced oxidation method. Moreover, for the first time, the volatilized emissions of VOCs were investigated and controlled to achieve the maximum VOC removal percent without generating any secondary pollution. Furthermore, the influence of various operating conditions, such as applied current and electrolyte concentration, on the removal of VOCs were systematically investigated. In addition, the optimum conditions for VOCs treatment and for the energy consumption of electrochemical advanced oxidation were evaluated. Finally, the effect of different catalysts from PGMs (namely Ir/Ti, Ir-Pt/Ti, Ir-Pd/Ti, and Ir-Ru/Ti) on VOCs removal was investigated to determine the optimum conditions for electrochemical advanced oxidation.

4.2 Materials and methods

4.2.1 Wastewater and chemicals

Artificial wastewater was synthetized in the laboratory by mixing 150 mg/L of chloroform (99.5%), benzene (99.5%), trichloroethylene (99.0%), and toluene (99.5%), which were supplied by Sam-Chun Pure Chemical Co., Ltd (Republic of Korea). Sodium chloride (99.5%), purchased from Junsei Chemical Co., Ltd (Japan), was used as the supporting electrolyte at 0.05 M. The prepared artificial wastewater was stirred at 300 rpm for 12 h before beginning the experiment in order to achieve a homogenous resolution of the VOCs in the synthesized water. The physicochemical information of VOCs is summarized in Table 4.1.

Table 4.1. Physicochemical characteristic of targeted VOCs.

Chemical	Molecular weight (g/mol)	Solubility (g/L)	Specific weight	Vapor pressure (mmHg)	Boling point (°C)	octanol-water partition coefficient
Chloroform ($CHCl_3$)	119.38	8.00	1.48	159.0	62.0	1.97
Benzene (C_6H_6)	78.11	1.80	0.88	94.8	80.1	2.13
Trichloroethylene (C_2HCl_3)	131.39	1.28	1.46	69.0	87.2	2.61
Toluene (C_7H_8)	92.14	0.53	0.86	28.4	111.0	2.73

4.2.2 Electrode materials

The anode and cathodes were designed to have surface areas of 50 cm^2 (7.1 cm in length, 7.1 cm in width, and 0.1 cm in thickness) with fifteen holes (⌀ = 6 mm) to enhance the VOC diffusion in the wastewater solution. The anode was made of a punctured Ti plate coated with a 3.0 μm-thin layer of different catalytic PGMs (Ir, Ir-Pt, Ir-Pd, and Ir-Ru). As the base model catalyst, Ir was used for its high chemical stability, with a weight of 90% of the total manufactured with the assistance of WESCO Electrodes Co. Ltd. (Republic of Korea).

4.2.3 Electrochemical reactor setup and operation

All the experiments were conducted in a rectangular reactor made from an acrylic sheet (74 × 46 × 110 mm). The distance between the anode and cathode materials was maintained at 2 mm. A simplified diagram of the experimental setup is shown in Fig. 4.1.

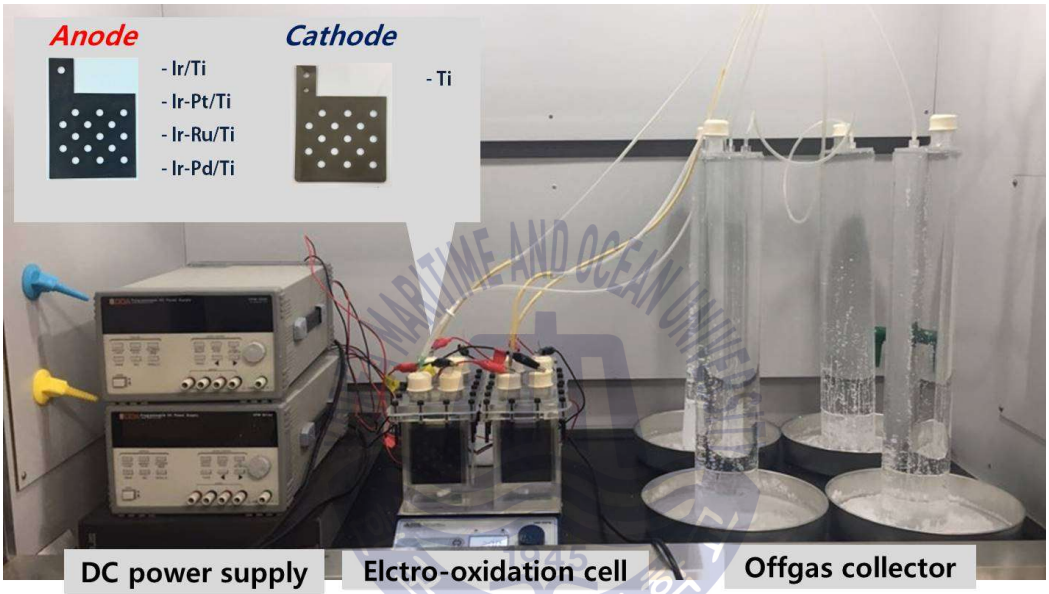

Fig. 4.1. The electrochemical advanced oxidation system for oxidizing VOCs and collecting generated gas (Batch type, 300 mL of working volume).

First, 300 mL of the synthetic (artificial) wastewater was inserted into the electrolysis cell and mixed using a magnetic stirrer to ensure the continuous dissolving of the VOCs in the solution during the experiment. Then, the cell was sealed with a cover, and the two electrodes were connected to a DC power supply, OPM-303D from ODA Co. (Republic of Korea), which was used for maintaining the current density at 25 mA/cm^2 during the electrochemical advanced oxidation. Also, the cell-voltage behavior was investigated and reordered using a millimeter device. To check the

treatment performance of the electrochemical advanced oxidation with regard to the VOC removal from the wastewater solution, the liquid samples were collected at 0, 15, 30, 45, 60, 90, and 120 min during the experiment. Moreover, the gases, such as H_2, O_2, and CO_2, produced by the VOC volatilization were collected using a cylindrical gas collector.

4.2.4 Measurements and calculations

The concentrations of VOCs in both the liquid and gas phases were analyzed using gas chromatography (GC) (Claus 580, PerkinElmer) with a flame ionization detector (FID, PerkinElmer) and a non-polar capillary GC column (Ultra-2, 25 m, 0.20 mm, Agilent). The condition of the GC characterization is shown in Table 3.1. The VOCs in the gas phase were injected directly into the GC analyzer; however, a headspace sampler (Turbo matrix 40, Perkin Elmer) was used to pretreat the liquid-phase VOCs before injection into the GC analyzer.

The actual amount of VOCs removed from wastewater solutions during electrochemical advanced oxidation can be calculated from the following equation:

$$X_r = X_O + X_V + X_U \tag{16}$$

where X_T is the total mass fraction (%), X_O is the oxidized mass fraction of electrochemical anodic reaction (%), X_V is the unoxidized but naturally volatilized mass fraction (%) and X_U is the untreated, remained mass

fraction (%) for the VOC components in the wastewater solution. X_T , X_V and X_U are known values; X_T can be calculated from the initial VOC concentration in the wastewater solution, X_V can be measured from the VOC concentration in the gas phase, and X_U can be calculated from the final VOC concentration in the wastewater solution after completing the experiment. X_O is the only unknown value, so it must be calculated from equation (16).

The energy consumption for oxidizing a unit mass of VOCs was calculated according to equation (17). Where EC is the energy consumption (kWh/g), $\triangle V$ is the average voltage (V), I is the current (A), t is the time of the electrochemical advanced oxidation process, and m_O is the mass of the oxidized VOCs.

$$EC = 1000 \times (\triangle V \times I \times t) / m_O \quad (17)$$

4.2.5 Material characterization of DSAs

The morphology of the DSAs was studied using an imaging SU70 (Hitachi, Japan) high-resolution field-emission scanning electron microscope (FE-SEM) equipped with an on-system energy dispersive X-ray spectroscopy (EDX) working at 5.0 kV. The surface area of the DSAs was determined using the Brunauer Emmett Teller (BET) analysis method with an ASAP 2010 analyzer (Micromeritics, US). The components of the anodes were measured using x-ray diffraction (Empyrean, PANalytical, Netherlands), operating at a voltage of 40 kV and a tube current of 30 mA, in the 2 theta range of 10

to 90 with increments of 0.013. Moreover, the wettability of the different anodes was measured, where the sessile drop method was used to measure the water contact angle of the anodes using DROP image Standard Device (Version 2.4). Where about 3 μL of deionized water was dropped onto the anode surface and the value of water contact angle was recorded at room temperature.

4.3 Results and discussion

4.3.1 Effect of operating conditions

1) Removal efficiency of VOCs based on time

Fig. 4.2 displays the removal efficiency of different VOC pollutants based on time; the results show that the Ir/Ti anode achieved excellent removal performance (>70%) for all investigated VOCs, in particular the toluene compound, which showed the highest removal efficiency in comparison with the others. The removal percentages were 98.7, 95.1, 84.8, and 79.6% for toluene, trichloroethylene, benzene, and chloroform, respectively. This high removal efficiency is attributed to the high oxygen evolution potential of 2.0 V and the high electrocatalytic activity of the Ir/Ti anode (Anglada et al., 2009). The high oxidation potential increased the anodic active site (oxidizing agents), which resulted in a highly selective oxidization reaction in the VOCs on the anode surface. However, the variation in the removal percentage from one pollutant to another is related to the change in chemical structure and the bond strengths. For example, chloroform has multiple single bonds between the C, Cl, and H atoms, and these strong bonds obstruct the oxidation reaction in the active site on the anode surface and decrease the attraction ability of the •OH site to the VOC

pollutants, while toluene compounds, in contrast, have weak double bonds, which means that it oxidizes rapidly and easily (Criddle and McCarty, 1991).

In Fig. 4.2, the significant effect of the operation time on the removal efficiency is notable. From the starting time to 60 min, the removal rate for all VOCs increased rapidly according to the same trend, which is attributed to the amount of VOCs content reaching the electrode surface at the beginning of the reaction; thus, the rate of decomposition continued along the same high trend until 90 min. However, after this point, the removal remained constant due to the volatilizations of VOC molecules from the wastewater solution. Overall, the results indicate that the optimum time for the maximum removal of VOCs is from 80–100 min.

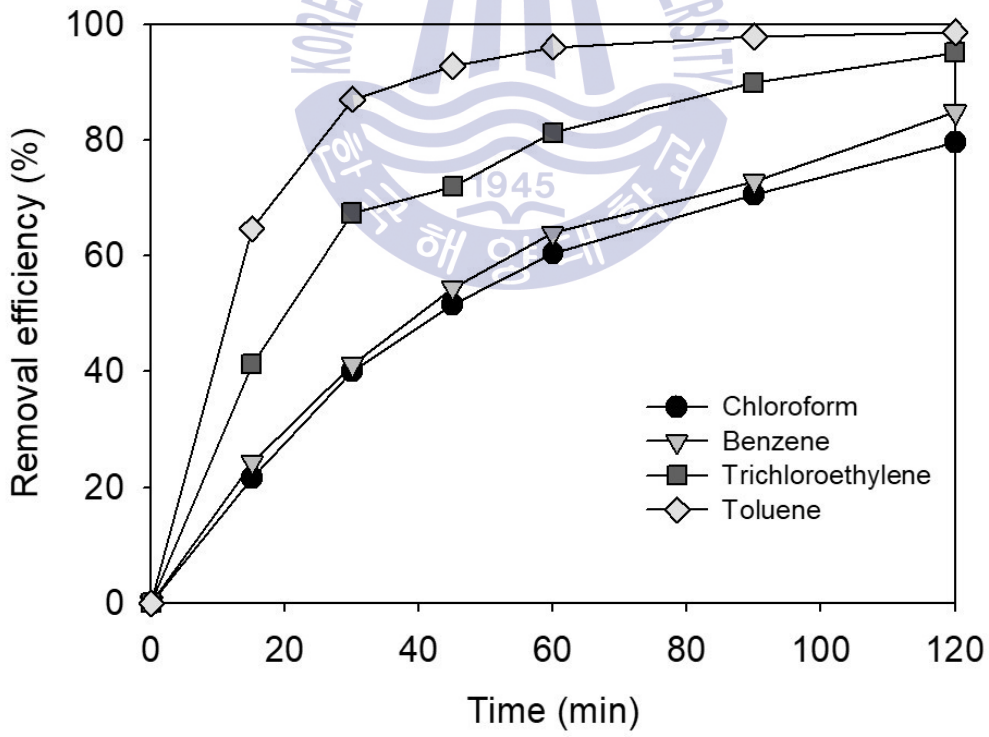

Fig. 4.2. Variation of each VOCs removal efficiency versus time at 25 mA/cm^2

and 0.05 mg/L NaCl (150 mg/L of initial VOCs concentration).

2) Effect of current density

Three characteristics (oxidized fraction, volatilized fraction, and energy consumption) were considered to investigate the optimum current density for the electrochemical advanced oxidation treatment of VOCs. Fig. 4.3a shows the effect of the current density, in a range from 20 to 45 mA/cm2, on chloroform removal from wastewater (as the most refractory compound of targeted VOCs) at 0.05 M NaCl. As shown in the figure, increasing the current density from 20 to 25 mA/cm^2 increased the oxidized fraction percent from 52.9% to 74.6%. This increase is attributed to the enhancement of the electron transfer process and the increase in the concentration of generated •OH groups on the anode surface (Niu et al., 2016).

However, it is apparent that after 30 mA/cm^2, increasing the current has only a slight effect on the removal efficiency. It can be assumed that at this current the more supporting electrons enhances the electrolysis process of H2O, which generates oxygen instead of the hydroxyl radical group; as a result, little improvement can be achieved. For example, the oxidized mass fraction increased by only 3 degrees when the current density was increased 1.5 times.

On the other hand, increasing the current density led to an increase in the temperature of the wastewater as a result of converting electrical energy, supported by the current density, into thermal energy in the water (Zhang et al., 2013). Because of the temperature increase from 36.0 to 62.0 ℃, the volatilized fraction increased from 5.1% at 20 mA/cm^2 to 13.3% for toluene pollutants. This rapid volatilization back to low boiling points and high vapor pressure in the VOCs is shown in Table 4.1.

Fig. 4.3b shows the energy consumed in oxidizing 1 g of chloroform at different current densities. It is observed from the figure that along with increasing the applied current density, it increased the energy consumption but decreased the operation time of the process. Therefore, the most effective and economic condition for optimum energy consumption was current density 25 mA/cm^2. It is worth mentioning that a higher current density leads to increased energy dissipation and a shorter electrode lifetime. Therefore, selecting a suitable current density for EAOPs treatment in practical applications is of great significance.

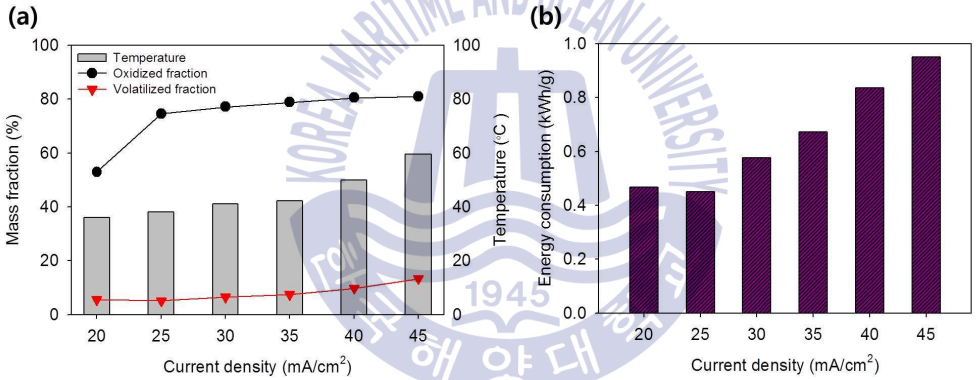

Fig. 4.3. Effects of current density on chloroform electrochemical advanced oxidation at 0.05 mg/L NaCl as electrolyte (150mg/L of initial concentration): (a) oxidized/volatilized fraction and temperature, (b) energy consumption to oxidize 1 g of chloroform.

3) Effect of electrolyte concentration

The effect of NaCl concentration (0.01–0.15 M) on the oxidized and volatilized VOC removal efficiency at the optimum current density of 25 mA/cm^2 is illustrated in Fig. 4.4. The maximum oxidized mass percentage of 79% was achieved at low electrolyte concentration yields (0.01–0.05 M). Moreover, the percentage tended to decrease as the electrolyte concentration increased up to 0.05 M because, in a fixed current density condition, the applied current is consumed to oxidize the pollutants and participate in side reactions simultaneously. Side reactions in electrochemical advanced oxidation include oxidizing electrolytes, agents on the anode surface, or •OH, all of which can diminish oxidation of VOC pollutants. However, the low-electrolyte solution led to reduced conductivity in the solution, which caused a high transfer resistance of the generated electrons to the anode surface and the electrolyte solution. This high resistance caused the anode temperature to rise, which in turn increased the volatile fraction of the VOCs. For example, the volatilized fraction decreased from 14.9 to 9.8% as the electrolyte concentration increased from 0.01 to 0.025 mg/L. From the results in Fig. 4.4, the optimum concentration of the supporting electrolyte for enhancing the removal percentage for both oxidized and volatilized VOCs is 0.05 mg/L.

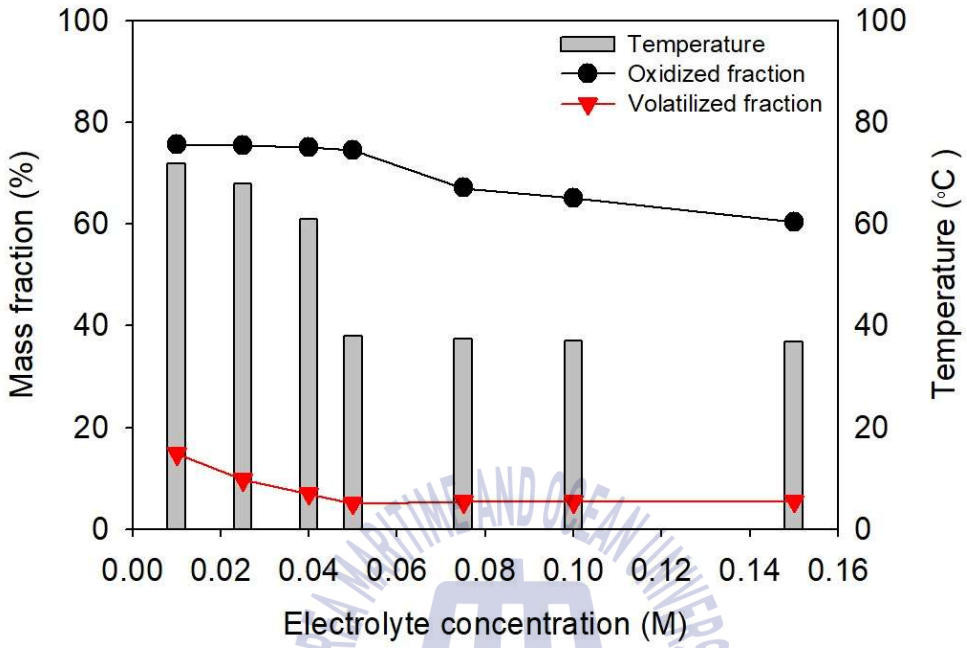

Fig. 4.4. Effects of electrolyte concentration on temperature and mass fraction of chloroform electrochemical advanced oxidation at 25 mA/cm^2 and 150 mg/L of initial concentration.

4.3.2 Determination of optimum DSA

1) Characterization of different DSAs in VOC removal performance

Fig. 4.5 displays the morphology of the different DSAs using SEM characterization. The clear roughness morphology of the surface area in the case of the Ir-Pd/Ti anodes increased the surface area, which led to an enhanced reaction in the active sites of the anodes which contrasts with the morphology in Ir-Pt/Ti and Ir-Pd/Ti anodes, respectively, where cracks totally covered the anodes' surface areas, as there is no doubt that this

cracking decreased the active sites on the anode surface, which led to decelerated oxidation reactions in the VOC organic pollutants.

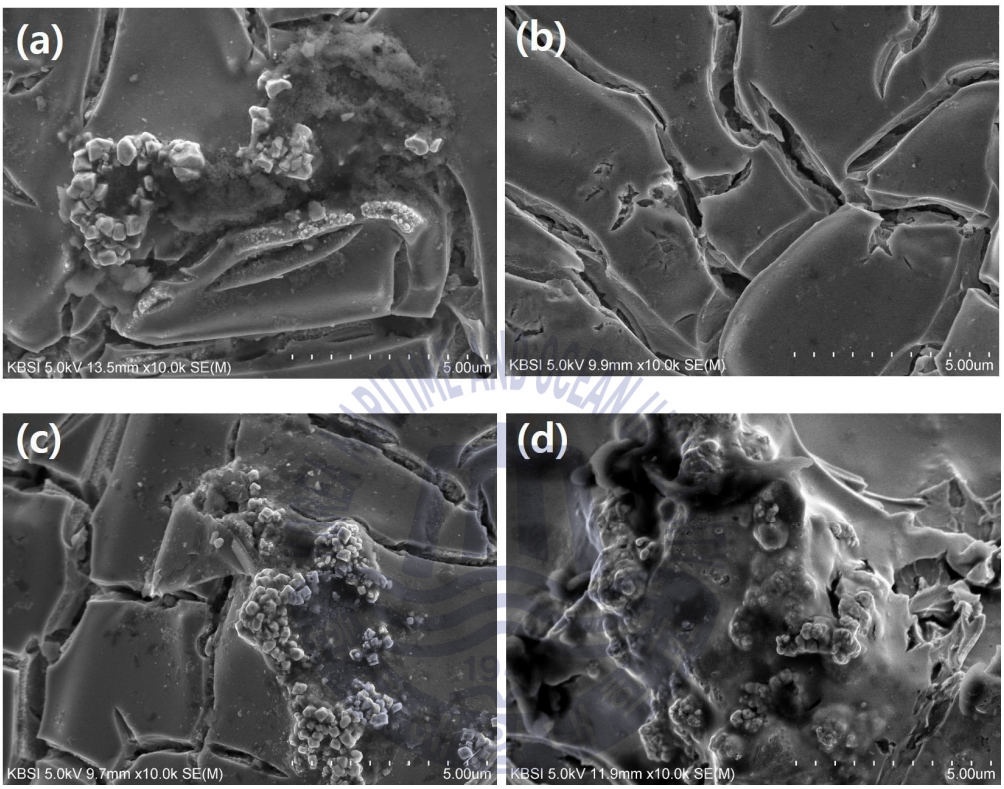

Fig. 4.5. Scanning electron microscope (SEM) images of (a) Ir/Ti, (b) Ir-Pt/Ti, (c) Ir-Ru/Ti, (d) Ir-Pd/Ti.

The BET characterizations results confirm that the surface area with Ir-Pd/Ti was the largest, as the surface areas were 0.5632, 0.5351, 0.4788, and 0.303 m^2/g for Ir-Pd/Ti, Ir-Ru/Ti, Ir-Pt/Ti, and Ir/Ti, respectively, as shown in Table 4.2. Moreover, Fig. 4.6 shows the XRD patterns for the electrodes, and the appearance peaks at 2 theta 35.09, 38.38, 40.17, 52.98,

62.96, 70.6, 76.21, and 77.36 are attributed to the pristine support material (Ti) corresponding to the (010), (002), (011), (012), (110), (013), (112), and (021) crystal planes. Based on the JCDPS database, the observed peaks at 27.9° , 39.9° and 39.7° confirmed the deposition of Ir, Pd, and Pt on the anode surface, where the peaks are attributed to the (111), (001), (011), and (013) planes, respectively. However, no peak appeared for Ru because of its amorphous structure. The water contact angles are 65° , 69° , 73° , and 76° for Ir-Pd/Ti, Ir/Ti, Ir-Pt/Ti, and Ir-Ru/Ti, respectively (See Fig. 4.7). The lowest hydrophobicity leads to the highest wetted surface area on the anode by the wastewater (electrolyte). Accordingly, active oxidation reaction rate was expected with the Ir-Pd/Ti, which minimizes the electron transfer resistance and enhances the active sites for VOC oxidation. Furthermore, the EDX analysis for the investigated anodes was completed, as shown in Fig. 4.8.

Table 4.2. Specific surface area of the manufactured DSAs.

Anode	Specific surface area (m^2/g)
Ir/Ti	0.3030
Ir-Pt/Ti	0.4788
Ir-Ru/Ti	0.5351
Ir-Pd/Ti	0.5632

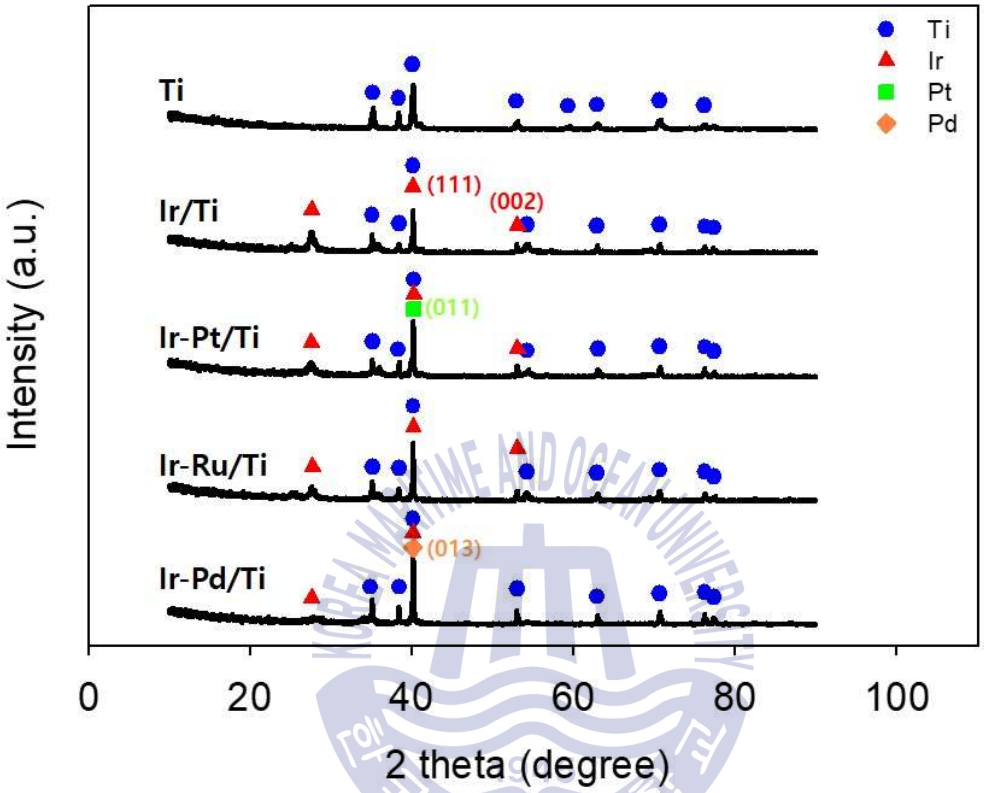

Fig. 4.6. x-ray diffraction (XRD) profiles of Ti, Ir/Ti, Ir-Pt/Ti, Ir-Ru/Ti and Ir-Pd/Ti.

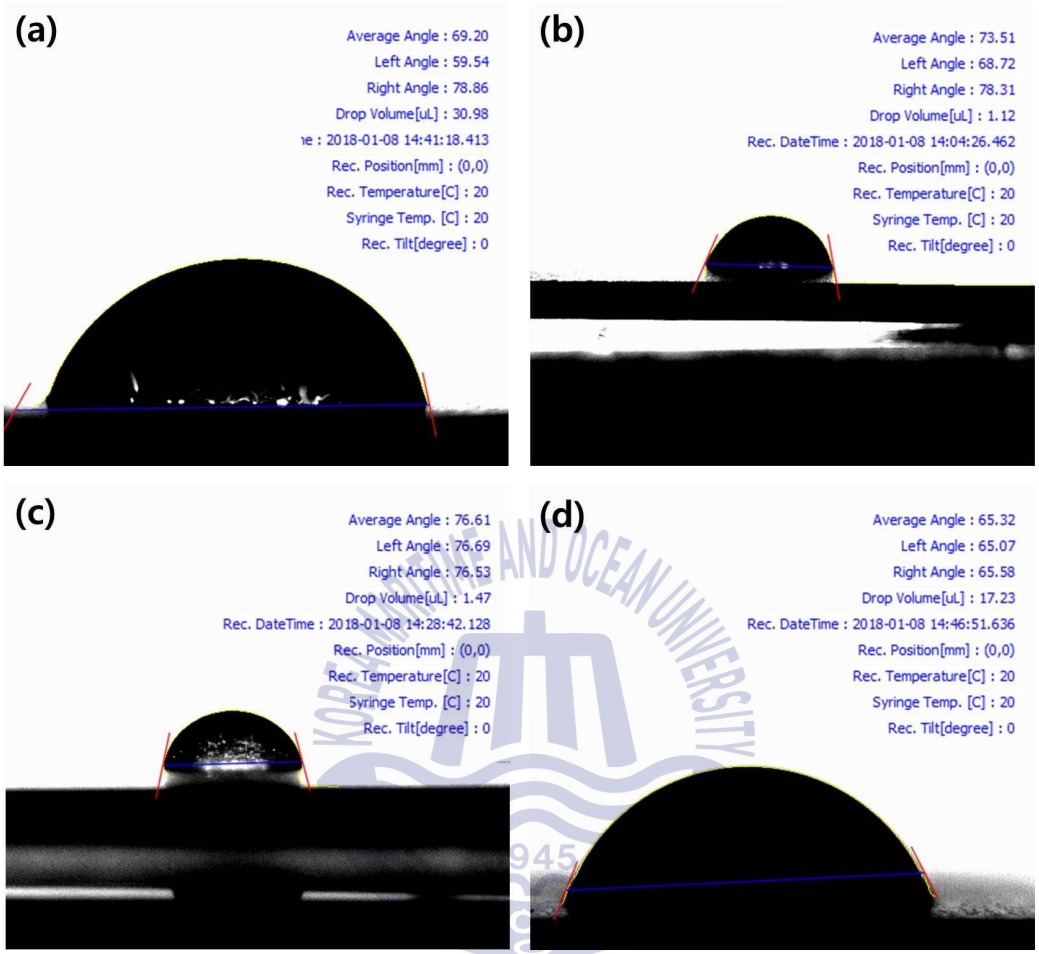

Fig. 4.7. Water contact angle of the manufactured DSAs: (a) Ir/Ti, (b) Ir-Pt/Ti, (c) Ir-Ru/Ti and (d) Ir-Pd/Ti.

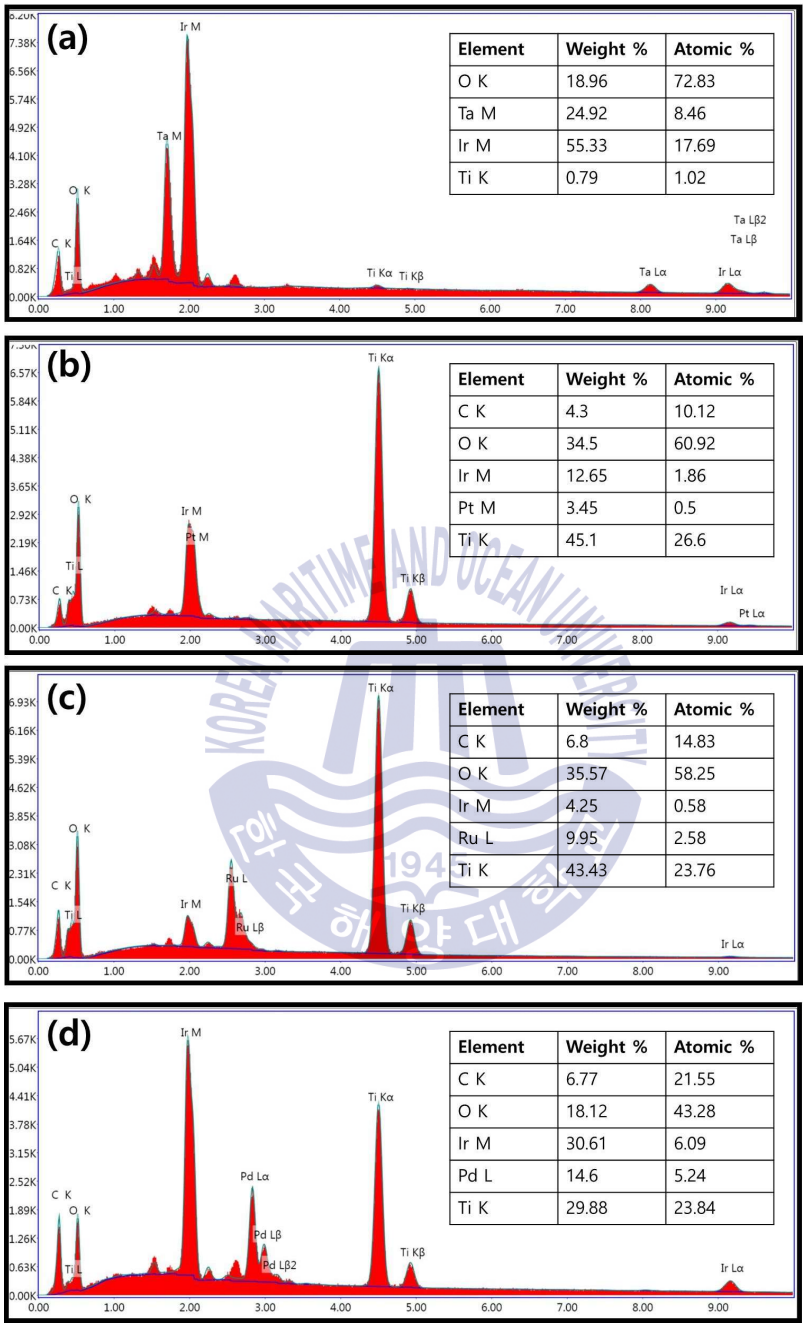

Fig. 4.8. Energy dispersive X-ray (EDX) spectra: (a) Ir/Ti, (b) Ir-Pt/Ti , (c) Ir-Ru/Ti, and (d) Ir-Pd/Ti.

2) Effect of different DSAs on VOC removal performance

The performance of different DSAs, such as Ir/Ti, Ir-Pt/Ti, Ir-Ru/Ti, and Ir-Pd/Ti, was investigated at 25 mA/cm^2 and 0.05 M NaCl, as optimum current density and electrolyte concentration for treating VOCs, respectively. As shown in Fig. 4.9, the Ir-Pd/Ti achieved the maximum removal efficiency for both oxidized and volatilized VOCs in comparison to the other electrodes; the obtained results were in the following order: Ir-Pd/Ti (83.2%) > Ir/Ti (79.6%) > Ir-Pt/Ti (68.8%) ≈ Ir-Ru/Ti (67.4%). The minimum volatilized percentages of VOCs were as follows: Ir-Pd/Ti (4.40%), Ir/Ti (5.07%), Ir-Pt/Ti (7.47%), and Ir-Ru/Ti (8.09%). These results confirm that Ir-Pd/Ti is the most promising anode for the removal of VOCs from wastewater solution. It was followed by Ir/Ti, Ir-Pt/Ti, and finally Ir-Ru/Ti. The high performance of the Ir-Pd/Ti anode was achieved due to its unique characteristics, such as high ·OH generation, its high wettability, high surface area, high crystal morphology, and excellent surface morphology. Additional experimental results from the various current densities are summarized at Table 4.3.

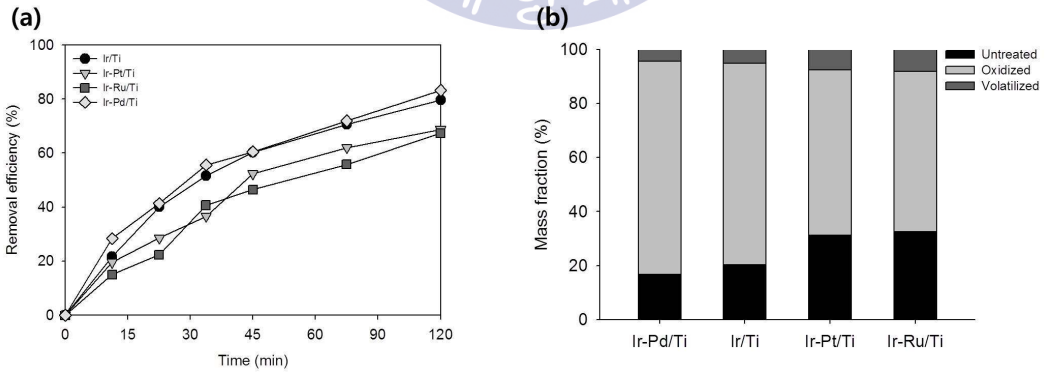

Fig. 4.9. Comparison of electrochemical advanced oxidation performance on different DSAs: (a) removal efficiency and (b) mass fraction (150 mg/L of initial chloroform concentration, 25 mA/cm^2 and 0.05 M NaCl).

Table 4.3. Oxidized and volatilized fractions of VOCs for different anodes and current densities at 0.05 M NaCl

Anode	Current density (mA/cm^2)	Temp. (℃)	Chloroform		Benzene		Trichloroethylene		Toluene	
			Oxidized fraction (%)	Volatilized fraction (%)	Oxidized fraction (%)	Volatilized fraction (%)	Oxidized fraction (%)	Volatilized fraction (%)	Oxidized fraction (%)	Volatilized fraction (%)
Ir/Ti	25	38	74.6	5.1	79.0	5.9	89.5	5.6	97.0	1.7
	35	42.2	78.8	7.4	82.8	8.0	92.2	6.2	97.1	2.5
	45	59.5	81.0	13.3	95.0	3.7	97.3	2.5	98.6	1.2
Ir-Pt/Ti	25	38.6	61.3	7.5	78.1	6.4	89.8	5.9	95.6	2.5
	35	43.7	75.2	7.8	87.2	6.3	92.2	6.1	96.6	2.8
	45	58.4	83.3	9.7	95.5	3.7	97.3	2.5	98.6	1.2
Ir-Ru/Ti	25	38	59.3	8.1	73.6	7.3	86.3	7.5	94.6	3.3
	35	44.5	74.3	8.9	86.7	5.7	92.7	6.2	95.9	3.3
	45	58	75.3	9.3	91.7	5.8	94.2	5.3	94.2	5.3
Ir-Pd/Ti	25	37	78.8	4.4	86.2	4.1	95.2	3.6	97.5	1.7
	35	42	79.1	5.0	89.7	5.1	95.7	3.7	97.8	1.8
	45	57.4	84.1	9.3	93.1	5.0	97.8	1.8	98.4	1.3

3) Energy consumption

The energy consumption of the anodes was calculated, as shown in Fig. 4.10. The results confirmed the effectiveness of Ir-Pd/Ti as a promising DSA. The energy consumption was the lowest in comparison to the other anodes. The energy consumption for treating 1 g of chloroform at 25 mA/cm^2 was 0.38, 0.45, 0.54, and 0.57 kWh for Ir-Pd/Ti, Ir/Ti, Ir-Pt/Ti, and Ir-Ru/Ti, respectively. In this study, chloroform was selected as an example of the most structurally strong bond VOC pollutants, so the other VOCs, such as benzene, trichloroethylene, and toluene, required lower energy consumption than chloroform (see Table 4.4). Also, it was confirmed that the application of a high current density was not economical because the treatment time was not reduced in proportion to the increase in current density.

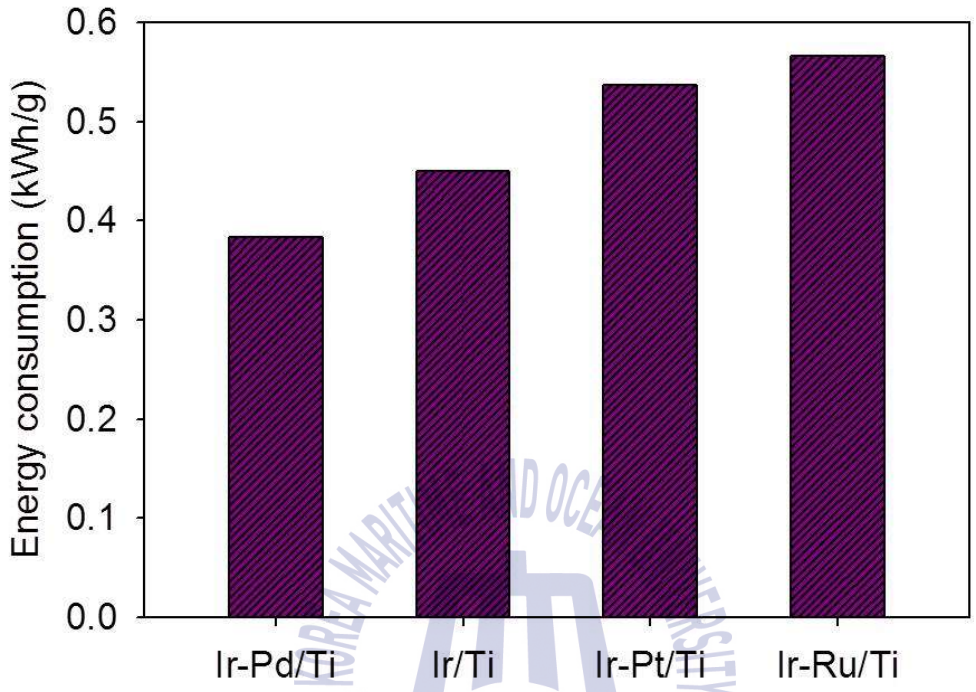

Fig. 4.10. Comparison of energy to oxidize mass of chloroform on different DSAs (150mg/L of initial concentration, 25 mA/cm^2 and 0.05 M as NaCl).

Table 4.4. Energy consumptions to oxidize 1g of each VOCs for different anodes and current densities at 0.05 M NaCl.

Anode	Current density (mA/cm^2)	Energy consumption (kWh/g oxidized removal)			
		Chloroform	Benzene	Trichloroethylene	Toluene
Ir/Ti	25	0.45	0.42	0.37	0.10
	35	0.67	0.64	0.57	0.16
	45	0.95	0.81	0.79	0.23
Ir-Pt/Ti	25	0.54	0.42	0.37	0.10
	35	0.72	0.62	0.59	0.17
	45	0.95	0.83	0.82	0.24
Ir-Ru/Ti	25	0.57	0.46	0.39	0.11
	35	0.70	0.60	0.56	0.16
	45	1.05	0.86	0.84	0.25
Ir-Pd/Ti	25	0.38	0.35	0.32	0.09
	35	0.62	0.54	0.51	0.15
	45	0.85	0.77	0.73	0.22

4.4 Conclusion

electrochemical advanced oxidation with various PGM catalysts was applied to treat VOCs, which are recalcitrant organics present in various industrial wastewaters. Evaluation of PGM composite DSAs and operating conditions were performed. Chloroform was determined to be the most refractory among the various VOCs tested. Determination of optimum conditions required assessment of proper current density and electrolyte concentration. Increased current density simultaneously increased oxidization and facilitated the volatilization derived from exothermic reactions. Moreover, at low electrolyte concentration, volatilization of VOCs from wastewater increased due to increased temperature whereas a high electrolyte concentration resulted in decreased oxidization of VOCs. As a result, the oxidation rate of VOCs increased proportionally up to a current density of 25 mA/cm^2, but the oxidation rate did not increase noticeably as the current density increased further. The optimum electrolyte concentration was determined to be 0.05 M as NaCl at a current density of 25 mA/cm^2. The Ir-Pd/Ti anode exhibited the best VOC oxidation ability, lowest VOC volatility, and lowest energy consumption used in oxidizing chloroform. electrochemical advanced oxidation with catalytic composite DSAs was a suitable process for removal of VOCs from wastewater. A stable and simple treatment with a volatilized fraction less than 5% was achieved. These results indicate that the side reaction activity and the degree of ClO^- generation are not significantly different among the DSAs, but the Ir-Pd/Ti electrode has the advantageous characteristics for ·OH generation. In addition, it is considered that the overall oxidative power influences the removal of VOC, rather than the selectivity of the oxidant.

Chapter 5. 1,4-dioxane wastewater treatment

5.1 Introduction

1,4-Dioxane is a commonly used substance in industrial processes, a highly flammable liquid with a flash point of 11 ℃ and is classified as a 2B class by international cancer research institutes. Korea Ministry of Environment reported that the load of dioxane occurred as much as 93.13% of the specific water pollutant load of 7457 kg/day in industrial wastewater (Korea Ministry of Environment, 2017). 1,4-Dioxane is not a biological treatment process unless specific microorganisms are established (Barajas-Rodriguez and Freedman, 2018). Furthermore, 1,4-dioxane is not suitable for adsorption treatment of activated carbon because of its high solubility (Barndõk et al., 2014). Because of these difficulties, some researchers are studying 1,4-dioxane using AOPs (Kwon et al., 2012). However, operating costs are known to be significant because of the need for strong oxidizing agents for 1,4-dioxane treatment (Barndõk et al., 2014).

To overcome these limitations, electrochemical advanced oxidation of 1,4-dioxane was attempted using DSAs and BDD anodes with different oxidant generating properties studied in chapter 3. The optimal electrode was selected by comparing the removal efficiency of 1,4-dioxane by the electrode and the power consumption. In addition, it was confirmed whether the specific oxidant was selectively involved in 1,4-dioxane treatment.

5.2 Materials and methods

5.2.1 Wastewater and chemicals

Artificial wastewater was synthetized in the laboratory by mixing 150 mg/L of 1,4-dioxane (99.5%), which were supplied by Sam-Chun Pure Chemical Co., Ltd (Republic of Korea). Sodium chloride (99.5%), purchased from Junsei Chemical Co., Ltd (Japan), was used as the supporting electrolyte at 0.05 M. The prepared artificial wastewater was stirred at 300 rpm for 12 h before beginning the experiment in order to achieve a homogenous resolution of the 1,4-dioxane in the synthesized water.

5.2.2 Electrode materials

The anode and cathodes were designed to have surface areas of 50 cm^2 (7.1 cm in length, 7.1 cm in width, and 0.1 cm in thickness) with fifteen holes ($\varnothing$ = 6 mm). The fabricated anode consists of three single catalytic DSAs, four composite catalytic DSA and BDD electrodes. The anode was made of a punctured Ti plate coated with a 3.0 μm-thin layer of different single catalytic PGMs (Ir, Pt and Ru) and composite catalytic PGMs (Ir-Pt, Ir-Ru, Ir-Pd and Ir-Pt-Pd). Each catalyst was used in an amount of 50 mg. As the base model of composite catalyst, Ir was used for its high chemical stability, with a weight of 90% of the total catalytic composites (45 mg of Ir and 5 mg of Pt, Pd, Ru or 2.5 mg of Pt and 2.5 mg of Pd respectively). Cathode was made of Pristine Ti. All the investigated electrodes were manufactured with the assistance of WESCO Electrodes Co. Ltd. (Republic of Korea).

5.2.3 Electrochemical reactor setup and operation

All the experiments were conducted in a rectangular reactor made from an acrylic sheet (74 × 46 × 110 mm). The distance between the anode and cathode materials was maintained at 2 mm. A simplified diagram of the experimental setup is shown in Fig. 4.1. First, 300 mL of the synthetic (artificial) wastewater was inserted into the electrolysis cell and mixed using a magnetic stirrer to ensure the continuous dissolving of the 1,4-dioxane in the solution during the experiment. Then, the cell was sealed with a cover, and the two electrodes were connected to a DC power supply, OPM-303D from ODA Co. (Republic of Korea), which was used for maintaining the current density at 25 mA/cm^2 during the electrochemical advanced oxidation. Also, the cell-voltage behavior was investigated and reordered using a millimeter device. To check the treatment performance of the electrochemical advanced oxidation with regard to the VOC removal from the wastewater solution, the liquid samples were collected at 0, 10, 20, 30, 45, 60, 90, and 120 min during the experiment.

5.2.4 Measurements and calculations

The concentrations of 1,4-dioxane in both the liquid and gas phases were analyzed using gas chromatography (GC) (Claus 580, PerkinElmer) with a flame ionization detector (FID, PerkinElmer) and a non-polar capillary GC column (Ultra-2, 25 m, 0.20 mm, Agilent). The condition of the GC characterization is shown in Table 3.1. A headspace sampler (Turbo matrix 40, Perkin Elmer) was used to pretreat the liquid-phase 1,4-dioxane before injection into the GC analyzer.

The energy consumption for oxidizing a unit mass of 1,4-dioxane was calculated according to equation (17).

5.3 Results and discussioins

5.3.1 Effect of different anodes on 1,4-dioxane removal performance

The performance of different DSAs, such as Ir/Ti, Ir-Pt/Ti, Ir-Ru/Ti, and Ir-Pd/Ti, was investigated at 25 mA/cm^2 and 0.05 M NaCl. As shown in Fig. 5.1, the BDD anode achieved the maximum removal efficiency in comparison to the other anodes; the obtained results were in the following order: BDD (95.8%) > Pt/Ti (90.3%) > Ir-Pd/Ti (31.0%) > Ru/Ti (22.0%) > Ir-Ru/Ti (21.4%) > Ir-Pt-Pd/Ti (20.8%) > Ir-Pt/Ti (19.5%) > Ir/Ti (14.0%). The result confirm that BDD is the most promising anode for the removal of 1,4-dioxane from wastewater solution. In addition, among the DSAs, Pt/Ti was found to be most suitable for 1,4-dioxane treatment. As shown in Fig. 3.5, the ·OH activity of each electrode is as follows : BDD/Ti > Pt/Ti > Ir-Pd/Ti > Ir-Pt-Pd/Ti > Ru/Ti > Ir-Ru/Ti > Ir-Pt/Ti > Ir/Ti. The removal efficiency of 1,4-dioxane was excellent for the BDD and Pt/Ti anodes, which had a much higher ·OH generation rate and lower ClO^- genereration rate. In addition, the removal efficiency of 1,4-dioxane was remarkably lowered in DSAs having a high degree of occurrence of ClO^- and a low degree of generation of ·OH. These results are due to the need for ·OH in the initial decomposition of 1,4-dioxane (Barndõk et al., 2014; Barndõk et al., 2016). Therefore, the high performance of the BDD anode was achieved due to its ·OH generation. However, even though the BDD electrode has more than twice the A generation rate compared to the Pt/Ti electrode, the treatment efficiency difference can not be followed. This phenomenon is considered to be caused by the reaction that all of the

generated ·OH is consumed in reactions such as generation of other ROS, not consumption of 1,4-dioxane.

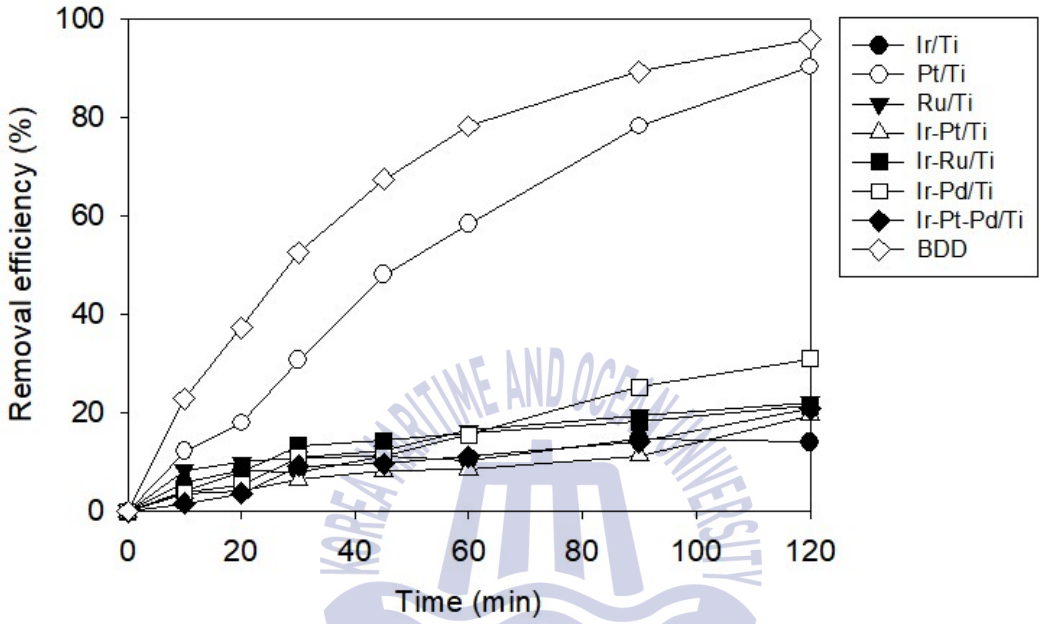

Fig. 5.1. Removal efficiency of 1,4-dioxane versus time on different anodes (150 mg/L of initial 1,4-dioxane concentration, 25 mA/cm^2 and 0.05 M NaCl).

5.3.2 Energy consumption

The energy consumption of the anodes was calculated, as shown in Fig. 5.2. The results confirmed the effectiveness of Pt/Ti. The energy consumption was the lowest in comparison to the other anodes. Although the treatment efficiency of the BDD anode is high, the phenomenon that the Pt/Ti electrode appears fine and efficiently appears as a difference in applied voltage. The electrochemical advanced oxidation with DSAs at 25 mA/cm^2 showed an applied voltage of 5.6-6.3 V, while the BDD electrode

showed 7.0-7.4. Therefore, the BDD electrode is inevitably disadvantageous in terms of power consumption unless the treatment efficiency is higher than 20%. In terms of 1,4-dioxane treatment, BDD electrodes differ in power consumption by less than 5%, while treatment rates differ by more than 5%. Therefore, it is reasonable to use BDD electrode in terms of process work except for electrode production cost.

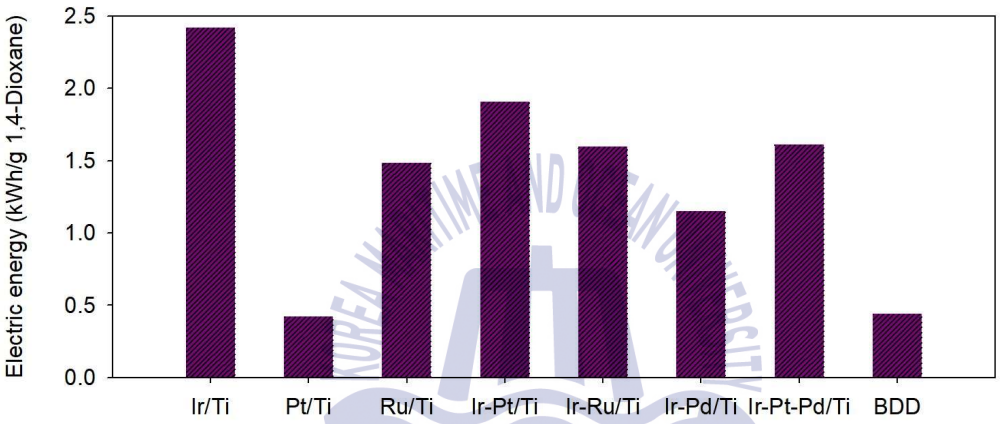

Fig. 5.2. Comparison of energy to removed mass of 1,4-dioxane on different anodes (150mg/L of initial concentration, 25 mA/cm^2 and 0.05 M as NaCl).

5.4 Conclusion

1,4-Dioxane was removed by the selectivity of the oxidant, unlike the VOCs materials discussed in chapter 4. The removal efficiency of 1,4-dioxane depends on the degree of ·OH generation of the anode. The removal efficiency of BDD and Pt/Ti electrode, which showed a high degree of ·OH generation, was 95% and 90%, respectively, while the other DSAs were less than 30%. However, ·OH ratio and the removal rate of 1,4-dioxane did not exactly coincide, presumably because ·OH was used for the production of ROS. When comparing the throughput and energy consumption, the BDD electrode appeared to be the most suitable for 1,4-dioxane removal. However, the production cost of BDD electrode is more than 4 times that of DSA electrode. Therefore, it is necessary to study the electrode using Pt material which has high ·OH generation rate in DSA.

Chapter 6. Conclusion

The side reaction activity and the oxidant generation rate of each kind of electrode were investigated using three kinds of single catalytic DSAs (Ir/Ti, Pt/Ti, Ru/Ti) and four kinds of composite catalytic DSAs (Ir-Pt/Ti, Ir-Ru/Ti, Ir-Pd/Ti and Ir-Pt-Pd/Ti) and BDD anode. Ru/Ti, Pt/Ti and BDD anodes showed low side reaction occurrence, whereas Ir/Ti and Ir based DSAs produced a lot of oxygen unnecessary for oxidant generation. However, the Ir-Pt-Pd/Ti electrode had less reactivity than the other Ir-based electrodes. The Pt/Ti and BDD electrodes had a small amount of ClO^-, but had an advantage of ·OH generation. On the other hand, DSAs except Pt/Ti have excellent ClO^- generation and ·OH generation ability. The Ir-based composite catalyst DSAs increased the oxidant generation compared to the Ir anode. Especially, the combination of the Pd catalyst with the Ir catalyst was found to help increase the degree of ·OH generation. Since the oxidant generation characteristics can be improved through the combination of various catalysts, a lot of research is required.

The removal efficiency of VOCs was evaluated by using Ir/Ti DSA and Ir-based catalyst DSAs (Ir-Pt/Ti, Ir-Ru/Ti and Ir-Pd/Ti). The optimum condition was selected considering the temperature condition and the removal efficiency for the volatilization prevention of VOCs. As a result, the electrolyte was 0.05 M NaCl and the current density was 25 mA/cm^2. The Ir-Pd electrode showed an excellent removal efficiency of 4-20% and a lower volatilization rate of 0.7-3.1% than the other electrodes. This is because Ir-Pd has a high degree of ·OH generation on the basis of a high hydrophilicity and surface area. In addition, the Ir-Pd electrode was found to have an advantage in terms of power consumption as well as

excellent processing efficiency. When the difference of VOCs removal efficiency is compared, it is considered that VOCs are eliminated by general oxidative power rather than oxidant selectivity.

The 1,4-dioxane removal efficiency of each kind of electrode were investigated using three kinds of single catalytic DSAs (Ir/Ti, Pt/Ti, Ru/Ti) and four kinds of composite catalytic DSAs (Ir-Pt/Ti, Ir-Ru/Ti, Ir-Pd/Ti and Ir-Pt-Pd/Ti) and BDD anode. BDD and Pt/Ti anodes showed more than 60% higher removal efficiency of 1,4-dioxane than other anodes. When the removal efficiencies of 1,4-dioxane were compared according to the types of electrodes, it is considered that the amount of generated ·OH greatly contributes to the decomposition mechanism.

Overall, DSAs were found to be able to improve the oxidant generation characteristics through changes in catalyst conditions. Since the characteristics of the oxidant generation according to the electrodes are different from each other, research on this is indispensable. Finally, depending on the removal mechanism of contaminants to be treated, it is necessary to use electrodes differently and to combine electrodes in various cases if necessary.

References

Ahmadzadeh, S., Asadipour, A., Pournamdari, M., Behnam, B., Rahimi, H.R., Dolatabadi, M., 2017. Removal of ciprofloxacin from hospital wastewater using electrocoagulation technique by aluminum electrode: Optimization and modelling through response surface methodology. Process Safety and Environmental Protection 109, 538-547.

An, C., Huang, G., Yao, Y., Zhao, S., 2017. Emerging usage of electrocoagulation technology for oil removal from wastewater: A review. The Science of the total environment 579, 537-556.

Anglada, A., Urtiaga, A., Ortiz, I., 2009. Contributions of electrochemical oxidation to waste-water treatment: fundamentals and review of applications. Journal of Chemical Technology and Biotechnology 84, 1747-1755.

Baddouh, A., Bessegato, G.G., Rguiti, M.M., El Ibrahimi, B., Bazzi, L., Hilali, M., Zanoni, M.V.B., 2018. Electrochemical decolorization of Rhodamine B dye: Influence of anode material, chloride concentration and current density. Journal of Environmental Chemical Engineering 6, 2041-2047.

Barajas-Rodriguez, F.J., Freedman, D.L., 2018. Aerobic biodegradation kinetics for 1,4-dioxane under metabolic and cometabolic conditions. Journal of Hazardous Materials 350, 180-188.

Barndõk, H., Cortijo, L., Hermosilla, D., Negro, C., Blanco, Á., 2014. Removal of 1,4-dioxane from industrial wastewaters: Routes of decomposition under different operational conditions to determine the ozone oxidation capacity. Journal of Hazardous Materials 280, 340-347.

Barndõk, H., Hermosilla, D., Han, C., Dionysiou, D.D., Negro, C., Blanco, Á., 2016. Degradation of 1,4-dioxane from industrial wastewater by solar

photocatalysis using immobilized NF-TiO2 composite with monodisperse TiO2 nanoparticles. Applied Catalysis B: Environmental 180, 44-52.

Basha, C.A., Chithra, E., Sripriyalakshmi, N., 2009. Electro-degradation and biological oxidation of non-biodegradable organic contaminants. Chemical engineering journal 149, 25-34.

Brillas, E., Garcia-Segura, S., Skoumal, M., Arias, C., 2010. Electrochemical incineration of diclofenac in neutral aqueous medium by anodic oxidation using Pt and boron-doped diamond anodes. Chemosphere 79, 605-612

Britto-Costa, P., Ruotolo, L., 2012. Phenol removal from wastewaters by electrochemical oxidation using boron doped diamond (BDD) and Ti/Ti0. 7Ru0. 3O2 dsa® electrodes. Brazilian Journal of Chemical Engineering 29, 763-773.

Cañizares, P., Gadri, A., Lobato, J., Nasr, B., Paz, R., Rodrigo, M.A., Saez, C., 2006. Electrochemical Oxidation of Azoic Dyes with Conductive-Diamond Anodes. Industrial & Engineering Chemistry Research 45, 3468-3473.

Carneiro, J.F., Aquino, J.M., Silva, A.J., Barreiro, J.C., Cass, Q.B., Rocha-Filho, R.C., 2018. The effect of the supporting electrolyte on the electrooxidation of enrofloxacin using a flow cell with a BDD anode: Kinetics and follow-up of oxidation intermediates and antimicrobial activity. Chemosphere 206, 674-681.

Celebioglu, A., Sen, H.S., Durgun, E., Uyar, T., 2016. Molecular entrapment of volatile organic compounds (VOCs) by electrospun cyclodextrin nanofibers. Chemosphere 144, 736-744.

Chae, K.J., Yim, S.K., Choi, K.H., Kim, S.K., Park, W.K., 2004. Integrated biological and electro-chemical treatment of swine manure. Water Science and Technology 49, 427-434.

Cheng, W.H., Hsu, S.K., Chou, M.S., 2008. Volatile organic compound emissions from wastewater treatment plants in Taiwan: legal regulations and costs of control. J Environ Manage 88, 1485-1494.

Chiang, L.-C., Chang, J.-E., Wen, T.-C., 1995. Indirect oxidation effect in electrochemical oxidation treatment of landfill leachate. Water Research 29, 671-678.

Cossu, R., Polcaro, A.M., Lavagnolo, M.C., Mascia, M., Palmas, S., Renoldi, F., 1998. Electrochemical treatment of landfill leachate: oxidation at Ti/PbO2 and Ti/SnO2 anodes. Environmental science & technology 32, 3570-3573.

Criddle, C.S., McCarty, P.L., 1991. Electrolytic model system for reductive dehalogenation in aqueous environments. Environmental Science & Technology 25, 973-978.

Curteanu, S., Godini, K., Piuleac, C.G., Azarian, G., Rahmani, A.R., Butnariu, C., 2014. Electro-oxidation method applied for activated sludge treatment: experiment and simulation based on supervised machine learning methods. Industrial & Engineering Chemistry Research 53, 4902-4912.

da Silva, A.J.C., dos Santos, E.V., de Oliveira Morais, C.C., Martínez-Huitle, C.A., Castro, S.S.L., 2013. Electrochemical treatment of fresh, brine and saline produced water generated by petrochemical industry using Ti/IrO2-Ta2O5 and BDD in flow reactor. Chemical Engineering Journal 233, 47-55.

Damalas, C.A., Eleftherohorinos, I.G., 2011. Pesticide exposure, safety issues, and risk assessment indicators. International journal of environmental research and public health 8, 1402-1419.

Domínguez, J.R., González, T., Palo, P. et al., 2012. Electrochemical Degradation of a Real Pharmaceutical Effluent. Water, Air and Soil Pollutio

n,223,2685-2694.

Dong, H., Zeng, G., Tang, L., Fan, C., Zhang, C., He, X., He, Y., 2015. An overview on limitations of TiO2-based particles for photocatalytic degradation of organic pollutants and the corresponding countermeasures. Water Research 79, 128-146.

Easter, C., Quigley, C., Burrowes, P., Witherspoon, J., Apgar, D., 2005. Odor and air emissions control using biotechnology for both collection and wastewater treatment systems. Chemical Engineering Journal 113, 93-104.

Fajardo, A.S., Seca, H.F., Martins, R.C., Corceiro, V.N., Freitas, I.F., Quinta-Ferreira, M.E., Quinta-Ferreira, R.M., 2017. Electrochemical oxidation of phenolic wastewaters using a batch-stirred reactor with NaCl electrolyte and Ti/RuO2 anodes. Journal of Electroanalytical Chemistry 785, 180-189.

Feng, L., Chang, J., Jiang, K., Xue, H., Liu, C., Cai, W.-B., Xing, W., Zhang, J., 2016. Nanostructured palladium catalyst poisoning depressed by cobalt phosphide in the electro-oxidation of formic acid for fuel cells. Nano Energy 30, 355-361.

Franz, J.A., Williams, R.J., Flora, J.R.V., Meadows, M.E., Irwin, W.G., 2002. Electrolytic oxygen generation for subsurface delivery: effects of precipitation at the cathode and an assessment of side reactions. Water Research 36, 2243-2254.

Gomes, A., Fernandes, E., Lima, J.L.F.C., 2005. Fluorescence probes used for detection of reactive oxygen species. Journal of Biochemical and Biophysical Methods 65, 45-80.

Hamida, S.B., Srivastava, V., Sillanpää, M., Shestakova, M., Tang, W.Z., Ladhari, N., 2017. Eco-friendly bleaching of indigo dyed garment by advanced oxidation processes. Journal of Cleaner Production 158, 134-142.

Hamza, M., Abdelhedi, R., Brillas, E., Sirés, I., 2009. Comparative electrochemical degradation of the triphenylmethane dye Methyl Violet with boron-doped diamond and Pt anodes. Journal of Electroanalytical Chemistry 627, 41-50.

He, H., Zhou, Z., 2017. Electro-Fenton process for water and wastewater treatment. Critical Reviews in Environmental Science and Technology 47, 2100-2131.

Jamaly, S., Giwa, A., Hasan, S.W., 2015. Recent improvements in oily wastewater treatment: Progress, challenges, and future opportunities. Journal of Environmental Sciences 37, 15-30.

Kanakaraju, D., Glass, B.D., Oelgemöller, M., 2018. Advanced oxidation process-mediated removal of pharmaceuticals from water: A review. Journal of Environmental Management 219, 189-207.

Khuntia, S., Majumder, S.K., Ghosh, P., 2015. Quantitative prediction of generation of hydroxyl radicals from ozone microbubbles. Chemical Engineering Research and Design 98, 231-239.

Korea ministry of environment, 2017. Occurrence and Treatment of Industrial Wastewater, 11-1480000-001452-10, 48-56.

Kwon, S.C., Kim, J.Y., Yoon, S.M., Bae, W., Kang, K.S., Rhee, Y.W., 2012. Treatment characteristic of 1,4-dioxane by ozone-based advanced oxidation processes. Journal of Industrial and Engineering Chemistry 18, 1951-1955.

Lee, J.Y., Lee, J.K., Uhm, S.H. and Lee, H.J., 2011. Electrochemical technologies : water treatement, Applied Chemistry for Engineeering, 22, 235-242.

Lee. K.J., Pyo, H.S., Yoo, J.K. and Lee, D.W., 2005. A study on removal of 1,4-dioxane in drinking water by multi filtration system, The Korean

Society of Analytical Science, 18, 154-162.

Liu, Z., Li, H., Li, M., Li, C., Qian, L., Su, L., Yang, B., 2018. Preparation of polycrystalline BDD/Ta electrodes for electrochemical oxidation of organic matter. Electrochimica Acta 290, 109-117.

López Peñalver, J.J., Gómez Pacheco, C.V., Sánchez Polo, M., Rivera Utrilla, J., 2013. Degradation of tetracyclines in different water matrices by advanced oxidation/reduction processes based on gamma radiation. Journal of Chemical Technology and Biotechnology 88, 1096-1108.

Mahajan, A., Banik, S., Roy, P.S., Chowdhury, S.R., Bhattacharya, S.K., 2017. Kinetic parameters of anodic oxidation of methanol in alkali: Effect of diameter of Pd nano-catalyst, composition of electrode and solution and mechanism of the reaction. International Journal of Hydrogen Energy 42, 21263-21278.

Ma, P., Ma, H., Galia, A., Sabatino, S., Scialdone, O., 2019. Reduction of oxygen to H2O2 at carbon felt cathode in undivided cells. Effect of the ratio between the anode and the cathode surfaces and of other operative parameters. Separation and Purification Technology 208, 116-122.

Martins, R., Britto-Costa, P.H., Ruotolo, L.A.M., 2012. Removal of toxic metals from aqueous effluents by electrodeposition in a spouted bed electrochemical reactor. Environmental technology 33, 1123-1131.

Moreira, F.C., Boaventura, R.A.R., Brillas, E., Vilar, V.J.P., 2017. Electrochemical advanced oxidation processes: A review on their application to synthetic and real wastewaters. Applied Catalysis B: Environmental 202, 217-261.

Mudliar, S., Giri, B., Padoley, K., Satpute, D., Dixit, R., Bhatt, P., Pandey, R., Juwarkar, A., Vaidya, A., 2010. Bioreactors for treatment of VOCs and

odours - a review. Journal of environmental management 91, 1039-1054.

Murillo-Sierra, J.C., Sirés, I., Brillas, E., Ruiz-Ruiz, E.J., Hernández-Ramírez, A., 2018. Advanced oxidation of real sulfamethoxazole + trimethoprim formulations using different anodes and electrolytes. Chemosphere 192, 225-233.

Nava, J.L., Sirés, I. and Brillas, E., 2014. Electrochemical incineration of indigo. A comparative study between 2D (plate) and 3D (mesh) BDD anodes fitted into a filter-press reactor, Environmental Science and Pollution Research, 21, 8485-8492.

Niu, J., Li, Y., Shang, E., Xu, Z., Liu, J., 2016. Electrochemical oxidation of perfluorinated compounds in water. Chemosphere 146, 526-538.

Palma-Goyes, R., Vazquez-Arenas, J., Torres-Palma, R., Ostos, C., Ferraro, F., González, I., 2015. The abatement of indigo carmine using active chlorine electrogenerated on ternary Sb 2 O 5-doped Ti/RuO 2-ZrO 2 anodes in a filter-press FM01-LC reactor. Electrochimica Acta 174, 735-744.

Panizza, M., Cerisola, G., 2009. Direct and mediated anodic oxidation of organic pollutants. Chemical reviews 109, 6541-6569.

Park, M.J., Lee, T.S., Kang, M.A and Han, C.B., 2016. The effect of pre-treatment methods for the life time of the insoluble electrodes, Journal of Korean Society of Environmental Engineers, 38, 291-298.

Pollack, I.B., Ryerson, T.B., Trainer, M., Neuman, J.A., Roberts, J.M., Parrish, D.D., 2013. Trends in ozone, its precursors, and related secondary oxidation products in Los Angeles, California: A synthesis of measurements from 1960 to 2010. Journal of Geophysical Research: Atmospheres 118, 5893-5911.

Pulgarin, C., Adler, N., Peringer, P., Comninellis, C., 1994. Electrochemical detoxification of a 1, 4-benzoquinone solution in wastewater treatment. Water Research 28, 887-893.

Rahmani, A.R., Godini, K., Nematollahi, D., Azarian, G., 2015. Electrochemical oxidation of activated sludge by using direct and indirect anodic oxidation. Desalination and Water Treatment 56, 2234-2245.

Ray, P.Z., Tarr, M.A., 2014. Solar production of singlet oxygen from crude oil films on water. Journal of Photochemistry and Photobiology A: Chemistry 286, 22-28.

Rivera-Utrilla, J., Gómez-Pacheco, C.V., Sánchez-Polo, M., López-Peñalver, J.J., Ocampo-Pérez, R., 2013. Tetracycline removal from water by adsorption/bioadsorption on activated carbons and sludge-derived adsorbents. Journal of environmental management 131, 16-24.

Sánchez-Carretero, A., Sáez, C., Cañizares, P., Rodrigo, M.A., 2011. Electrochemical production of perchlorates using conductive diamond electrolyses. Chemical Engineering Journal 166, 710-714.

Särkkä, H., Bhatnagar, A., Sillanpää, M., 2015. Recent developments of electro-oxidation in water treatment — A review. Journal of Electroanalytical Chemistry 754, 46-56.

Shah, M., 2004. Pervaporation?air stripping hybrid process for removal of VOCs from groundwater. Journal of Membrane Science 241, 257-263.

Sharma, K., Sharma, S., Sharma, S., Singh, P., Kumar, S., Grover, R., Sharma, P., 2007. A comparative study on characterization of textile wastewaters (untreated and treated) toxicity by chemical and biological tests. Chemosphere 69, 48-54.

Singla, J., Verma, A., Sangal, V.K., 2018. Parametric optimization for the

treatment of human urine metabolite, creatinine using electro-oxidation. Journal of Electroanalytical Chemistry 809, 136-146.

Vaghela, S.S., Jethva, A.D., Mehta, B.B., Dave, S.P., Adimurthy, S., Ramachandraiah, G., 2005. Laboratory Studies of Electrochemical Treatment of Industrial Azo Dye Effluent. Environmental Science & Technology 39, 2848-2855.

Van Hege, K., Verhaege, M., Verstraete, W., 2002. Indirect electrochemical oxidation of reverse osmosis membrane concentrates at boron-doped diamond electrodes. Electrochemistry Communications 4, 296-300.

Wu, C.H., Feng, C.T., Lo, Y.S., Lin, T.Y., Lo, J.G., 2004. Determination of volatile organic compounds in workplace air by multisorbent adsorption/thermal desorption-GC/MS. Chemosphere 56, 71-80.

Yavuz, Y., Koparal, A.S., 2006. Electrochemical oxidation of phenol in a parallel plate reactor using ruthenium mixed metal oxide electrode. Journal of hazardous materials 136, 296-302.

Yi, Z., Kangning, C., Wei, W., Wang, J. and Lee, S., 2007. Effect of IrO2 loading on RuO_2–IrO_2–TiO_2 anodes: A study of microstructure and working life for the chlorine evolution reaction, Ceramics International, 33, 1087-1091.

Zhang, C., Yu, Y., Grass, M.E., Dejoie, C., Ding, W., Gaskell, K., Jabeen, N., Hong, Y.P., Shavorskiy, A., Bluhm, H., Li, W.-X., Jackson, G.S., Hussain, Z., Liu, Z., Eichhorn, B.W., 2013. Mechanistic Studies of Water Electrolysis and Hydrogen Electro-Oxidation on High Temperature Ceria-Based Solid Oxide Electrochemical Cells. Journal of the American Chemical Society 135, 11572-11579.

Zollinger, H., 2003. Color chemistry: syntheses, properties, and applications of organic dyes and pigments. John Wiley & Sons.

Academic achievement

Peer-reviewed journal article (International)

1. **Wan-Cheol Cho**, Kyung-Min Poo, Hend Omar Mohamed, Tae-Nam Kim, Yul-Seong Kim, Moon Hyun Hwang, Do-Won Jung and Kyu-Jung Chae. "Non-Selective Rapid Electro-Oxidation of Persistent, Refractory Vocs in Industrial Wastewater Using a Highly Catalytic and Dimensionally Stable Ir-Pd/Ti Composite Electrode." Chemosphere 206, (2018): 483-490. (IF=4.427)
2. Eun-Bi Son, Kyung-Min Poo, Hend Omar Mohamed, Yun-Jeong Choi, **Wan-Cheol Cho** and Kyu-Jung Chae. "A Novel Approach to Developing a Reusable Marine Macro-Algae Adsorbent with Chitosan and Ferric Oxide for Simultaneous Efficient Heavy Metal Removal and Easy Magnetic Separation." Bioresource Technology 259, (2018): 381-387 (IF=5.807)

Peer-reviewed journal article (Domestic)

1. **조완철**, 부경민, 이지은, 김태남, 채규정, "전극의 부반응 기포발생에 따른 휘발특성과 전기화학고도산화능을 동시에 고려한 휘발성 유기화합물 처리용 최적 불용성전극 개발", 대한상하수도학회 (accepted)

Conference presentations (International)

1. **Wan-Cheol Cho**, Tae-Nam Kim, Kyung-Rok Kim, Kyung-Min Poo, In-Soo Kim, Do-Won Jung and Kyu-Jung Chae, Evaluation of VOCs removal performance using anodic oxidation with various platinum group catalysts, 2017 International Environmental Engineering Conference and Annual Meeting of the Korean Society of Environmental Engineers (IEEC 2017), Jeju, Korea, 15-17, Nov, 2017, p.255-256.
2. Sung-Gwan Park, **Wan-Cheol Cho**, Kyu-Jung Chae, Methanogen activity control with 2-bromoethanesulfonate (BES) and coenzyme M in microbial electrolysis cell for the production of electrobiofuels, The 15th IWA world conference on Anaerobic Digestion, Beijing, China, 17-20 Oct, 2017, p.71.

3. **Wan-Cheol Cho**, Kyung-Min Poo, Tae-Nam Kim, In-Soo Kim and Kyu-Jung Chae, Selection of suitable electrode for 1,4-dioxane wastewater treatment using DSAs and BDD electrode, Asia Pacific Society for Materials Research 2018 Annual Meeting (APSMR 2018 Annual Meeting), Hokkaido, Japan, 19-22 Jul, 2018.

Conference presentations (Domestic)

1. **조완철**, 김태남, 김동수, 김경록, 손은비, 부경민, 채규정, 친환경응집제와 미세기포를 이용한 2단막 배출수 부상분리특성 연구, 2016 대한환경공학회, 경주, 대한민국, 16-18 Nov, 2016, p.409-410.

2. 김동수, 안창효, 채규정, **조완철**, 김태남, 김경록, 이용수, 멀티보어형 분리막을 이용한 2단 막여과 공정에서 여과특성 연구, 2016 대한환경공학회, 경주, 대한민국, 16-18 Nov, 2016, p.407-408.

3. **조완철**, 박성관, 김태남, 부경민, 채규정, 복합촉매 DSA 전극을 이용한 유류폐수의 전기화학고도산화 처리, 2017 한국물환경학회, 광주, 대한민국, 23-24 Mar, 2017, p.755-756.

4. **조완철**, 박성관, 김태남, 부경민, 채규정, 복합촉매 DSA 전극을 이용한 유류폐수의 전기화학고도산화 처리, 대한상하수도학회・한국물환경학회 2017년 공동학술발표회, 광주, 대한민국, 23-24 Mar, 2017, p.755-756.

5. **조완철**, 김태남, 부경민, 김인수, 장재수, 채규정, BDD 전극과 복합촉매 DSA 전극을 이용한 1,4-다이옥산 함유폐수의 전기화학고도산화 처리, 한국물환경학회•대한상하수도학회 2018년 공동학술발표회, 일산, 대한민국, 22-23 Mar, 2017, p.192-193.

6. 김태남, **조완철**, 부경민, 김인수, 장재수, 채규정, 유해화학물질이 함유된 유류폐수의 급속처리를 위한 DSA와 BDD 전극의 적용 및 평가, 한국물환경학회・대한상하수도학회 2018년 공동학술발표회, 일산, 대한민국, 22-23 Mar, 2017, p.297-298.

7. **조완철**, 박성관, 천경호, 강문선, 김용학, 김승준, 채규정, 개도국 음용수 공급을 위한 이동식 무인 자동화 분리막 시스템, 2018년도 대한기계학회 부산지회 춘계학술대회, 11 May, 2018, p.6-7.

8. **조완철**, 김태남, 부경민, 손은비, 김인수, 채규정, 1,4-다이옥산 함유폐수의 전기화학적 고도산화 처리를 위한 Boron-doped diamond 전극과 Dimensionally stable anode의 특성 평가, 2018 대한환경공학회, 광주, 대한민국, 14-16 Nov, p.259-260.

Award

1. 학술연구발표회논문상, **조완철**, 김태남, 김동수, 김경록, 손은비, 부경민, 채규정, 친환경응집제와 미세기포를 이용한 2단막 배출수 부상분리특성 연구, 2017 대한환경공학회 국내학술대회, 제주, 대한민국, 15-17, Nov, 2017.

Patents

1. 채규정, 부경민, 박성관, **조완철**, 압력조절식 미세기포 가압부상분리 장치와 이를 이용하는 가압부상분리 방법 및 이들을 이용하는 수처리 시스템, 등록번호: 10-1877935, 07 Jul, 2018.
2. 채규정, **조완철**, 막 여과 배출수 처리 시스템 및 이를 이용하는 막 여과 배출수 처리 방법, 등록번호: 10-1909277, 11 Oct, 2018.

감사의 글

석사 과정을 시작하면서부터 졸업 논문을 완성하기까지 수많은 사람들의 도움을 받았습니다. 저를 이끌어주시고 함께한 모든 분들에게 이 자리를 빌려 감사의 말씀을 올립니다.

가장 먼저 많은 것을 경험하게 해주시고 아낌없는 지도와 관심을 가져주신 지도교수 채규정 교수님께 진심으로 감사드립니다. 또한, 가장 바쁜 시기에 논문의 심사를 맡아주신 송영채 교수님, 장재수 교수님께도 감사드립니다. 더불어 학부 과정과 석사 과정을 보내는 동안 많은 가르침을 주시고 환경공학과를 위해 끊임없이 노력해 오신 김인수 교수님, 고성철 교수님, 김명진 교수님께도 감사드립니다. 앞으로 여러 교수님들과 학과에 누가 되지 않도록 열심히 하겠습니다.

가족 같은 분위기 속에서 연구할 수 있도록 만들어주신 WENL 식구들에게 감사드립니다. 석사 생활의 멘토가 되어주신 부경민 박사님, 언제나 웃으며 저를 도와주신 이지은 박사님, Hend 박사님 감사합니다. 항상 많은 것을 배려해준 랩 매니저 성관이형, 휴일 가리지 않고 도와주던 태남이형, 졸업선배 경록이형, 같이 졸업하는 은비, 언제나 열심히인 윤정, Tasnim, 모두들 돌아보면 함께 있어주어서 감사합니다. 학부생부터 함께 해 온 많은 시간들을 잊지 않겠습니다. 앞으로도 즐겁게 연구하시고 부가적으로 많은 성과가 따라오기를 기원합니다.

또한, 학부를 시작하면서부터 석사 과정을 마치기까지 함께라서 의지가 된 준혁이와 나이는 저보다 어리지만 많은 것을 배울 수 있었던 석사 동기 채영이에게도 고마움을 표합니다.

대학원생들의 정신적 지주이신 태선이형을 포함하여 떨어져 있다는 이유로 자주 보지 못한 7층 환경공학과 선·후배 여러분께 감사드리고 언제나 실험하는데 불편함이 없도록 도움을 주신 온랩 최철림 사장님, 일을 대하는 태도 하나하나에서 많은 것을 배웠습니다.

무엇을 하던 믿어주시는 부모님과 늘 잘 될 것이라고 응원해주는 누나에게 감사하고 사랑한다는 말 남깁니다. 믿음과 응원에 보답할 수 있도록 노력하겠습니다.

이 외에도 미처 표현하지 못한 많은 분들께 감사드립니다. 여러 분의 도움을 받은 만큼 저도 어디에서 감사받는 사람이 되도록 노력하겠습니다.

다시 한 번 감사의 말씀을 드리며 이 글을 마칩니다.

2019년 1월

조완철 올림